

# Focal- $\pi$ Shaper\_Q

(L13020)

High efficient Beam Shapers for focused laser beams transforming Gaussian to Flat-top or Doughnut spot profiles

## Manual



Fig. 1 Focal- $\pi$ Shaper\_Q

July 19, 2024

## 1. Specification

Table 1

Common for all Focal- $\pi$ Shaper_Q models									
Description	Beam shaper, lossless transforming Gaussian beam to the beam with Airy disk profile to get Flat-top or Donut focused spots with minimized side-lobes								
Input beam	<ul style="list-style-type: none"> <li>• TEM<sub>00</sub>, typically M<sup>2</sup>&lt;1.5</li> <li>• Divergence within <math>\pm 20</math> mrad range</li> </ul>								
Transmission	>99% in the working spectral range								
Alignment	X / Y lateral translation, $\pm 2$ mm range								
Features									
Model	Input $\varnothing$ 1/e <sup>2</sup> , mm	max. CW power, W	Spectrum, nm	CA, mm	Dimensions, mm		Weight, g	Mounting threads	
					$\varnothing$	Length			
Focal- $\pi$ Shaper_1064									
_Q-3	2.5 - 4	100	1020-1100	20	42	29	50	M30x0.75 outer/inner	
_Q-4	3 - 5								
_Q-5	4 - 6								
_Q-7.5	6 - 9	200							
_Q-10	8 - 12								
_Q-14	11 - 17	300		38	64	21	70		<ul style="list-style-type: none"> <li>• M58x1 outer/inner</li> <li>• Adapter M30x0.75</li> </ul>
_Q-17	15 - 20	400							
_Q-20	18 - 23								
Focal- $\pi$ Shaper_1070									
_Q-5_HP	4 - 6	1500	1020-1100	20	42	29	50	M30x0.75 outer/inner	
_Q-7.5_HP	6 - 9	2000							
_Q-10_HP	8 - 12	3000							
_Q-17_HP	15 - 20	4000		38	64	21	70		<ul style="list-style-type: none"> <li>• M58x1 outer/inner</li> <li>• Adapter M30x0.75</li> </ul>
_Q-20_HP	18 - 23	5000							
Focal- $\pi$ Shaper_NIR									
_Q-3	2.5 - 4	100	1500-2100	20	42	29	50	M30x0.75 outer/inner	
_Q-4	3 - 5								
_Q-5	4 - 6	200							
_Q-7.5	6 - 9								
_Q-10	8 - 12								
Focal- $\pi$ Shaper_TIS									
_Q-3	2.5 - 4	100	750 - 900	20	42	29	50	M30x0.75 outer/inner	
_Q-4	3 - 5								
_Q-5	4 - 6	200							
_Q-7.5	6 - 9								
_Q-10	8 - 12								
_Q-14	11 - 17	300							
Focal- $\pi$ Shaper_NUV									
_Q-3	2.5 - 4	100	335 - 560	20	42	29	50	M30x0.75 outer/inner	
_Q-4	3 - 5								
_Q-5	4 - 6	200							
_Q-7.5	6 - 9								
_Q-10	8 - 12								
Focal- $\pi$ Shaper_266									
_Q-3	2.5 - 4	100	250 - 275	20	42	29	50	M30x0.75 outer/inner	
_Q-4	3 - 5								
_Q-5	4 - 6	200							
_Q-7.5	6 - 9								
_Q-10	8 - 12								
Focal- $\pi$ Shaper_CO2									
_Q-5	4 - 6	200	9 – 11 $\mu$ m	20	42	29	50	M30x0.75 outer/inner	
_Q-7.5	6 - 9								
_Q-10	8 - 12								

## 2. Description

The series of beam shapers *Focal- $\pi$ Shaper\_Q* present optical tools for manipulating the intensity profile in a spot of a focused beam. The principle of operation, presented in Fig. 1, involves the conversion of a single mode ( $TEM_{00}$ ) laser beam into a beam with the "Airy Disk" intensity distribution; further focusing of this output beam using a diffraction limited lens or optical system results in spots of various intensity distributions in area near the lens focus: Flat-top, Donut-like, Inverse Gaussian, etc. Because of many identical features, the generic name *F- $\pi$ Shaper* is used, if necessary, differences between models will be noted additionally.

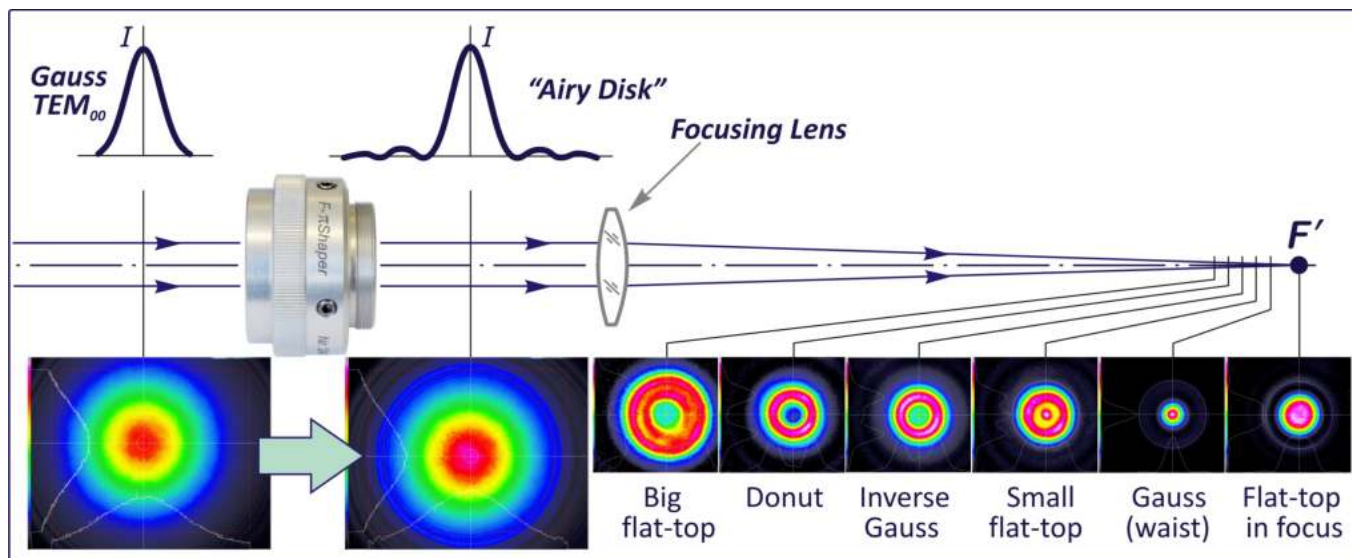


Fig. 2 The principle of operation of the *Focal- $\pi$ Shaper\_Q* with examples of measured profiles.

Most important features and basic principles of *F- $\pi$ Shaper*:

- refractive optical systems transforming the Gaussian to Airy Disk intensity distribution;
- flat-top, doughnut, inverse-Gauss and other profiles can be generated by the same device;
- operation with input  $TEM_{00}$  beams, typically  $M^2 < 1.5$ ;
- operation in a certain spectral band;
- systems optimized for other wavelengths are available as well;
- integrated X/Y alignment: lateral translations,  $\pm 2$  mm range;
- easy integration in a laser system;
- any diffraction limited focusing lens or complex optical system can be applied;
- wide range of distances between the *Focal- $\pi$ Shaper* and the lens.

Typical applications:

- 3D Printing – Laser Powder Bed Fusion (L-PBF)
- Microwelding
- Drilling
- Patterning
- Micromachining
- Scribing
- Cutting
- Solar Cell Processing

### 3. Input Beam

The optical design of the  $F\text{-}\pi\text{Shaper}$  assumes that the input beam is  $\text{TEM}_{00}$  with  $M^2 < 1.5$ , that is, it has a common wavefront, see examples in Fig.2. The input beam can be not only *collimated*, which is preferable, but also *divergent* or *convergent* with a divergence angle in the range of  $\pm 20$  mrad.

Owing to the principle of operation, the  $1/e^2$  intensity beam diameter  $2\omega$  ( $\omega$  is the beam waist) is pre-determined for each model, the exact data are given in Table 1.

The Clear Apertures of the  $F\text{-}\pi\text{Shaper}$  are more than 2 times larger than the optimum  $2\omega$ ; therefore, without taking into account the reflection losses, theoretically  $>99.9\%$  of a Gaussian beam is guaranteed to pass through the optics.

*Notes: Variation of the input beam size results in a variation of output profile!*

*Deviation of the input beam profile from the Gaussian function also results in a variation of the output profile!*

*To evaluate the intensity distribution, it is highly recommended to use dedicated instruments, for example, camera-based beam profilers!*

*Do not use the Scanning Slit beam profilers!*

The dependence of the resulting profiles near the focal plane on the size of the input beam is presented in the Chapter 5 "Focusing of the Output Beam". When building optical systems with  $F\text{-}\pi\text{Shaper}$ , it is highly recommended that the diameter of the input beam can be adjusted with control of the output beam and profiles in a focused spot. Resizing of the input beam size can be realized using a zoom beam expander, another recommended method is the use of a negative lens with an air gap between the laser and the  $F\text{-}\pi\text{Shaper}$ , see the p.4.3 in the paper in Appendix 2. At the alignment stage, see sections 10 and 11.2, it is recommended to provide an input beam of maximum diameter, and then the beam shaping effect will be most pronounced, which simplifies the alignment process and makes it more reliable. At a late stage of the adjustment procedure, it is necessary to tune the input beam diameter to ensure the optimum profile with minimized side-lobes in the working spot.

$F\text{-}\pi\text{Shaper}$  is developed to work with variety of  $\text{TEM}_{00}$  lasers: Nd:YAG, Fiber Laser, Diode lasers, and other lasers in the UV, visible and near-IR spectra. Recommended maximum power specifications are given in Table 1.

Due to the principle of operation, the  $F\text{-}\pi\text{Shaper}$  models are optimized for specific spectral bands given in Table 1 and in Chapter 6 "Spectral properties". Using  $F\text{-}\pi\text{Shaper}$  outside the optimal spectrum will result in increased losses and reduced performance.

### 4. Output Beam

In accordance with the principle of operation, which implies optimization of the interference conditions when focusing the beam, the output beam has an intensity profile described by the "Airy Disk" function or close to this function: a bright round central region is surrounded by a series of concentric rings of relatively low intensity. A detailed description of the Airy disk function can be found in the special literature on the effects of optical diffraction. An example of a real intensity pattern after the  $F\text{-}\pi\text{Shaper}$ , in the case of the maximum input beam size recommended in Table 1, is presented in Fig.2; compare the measured input and output profiles, the first concentric ring is very clearly visible.

Since  $F\text{-}\pi\text{Shaper}$  are afocal optical systems with  $\sim 1^X$  magnification, the divergence angle and the size of the output beam remain the same as at the  $F\text{-}\pi\text{Shaper}$  input.

The structure of the output profile remains stable over long distances, usually more than 1 meter. With propagation in space, the contrast of the concentric pattern becomes higher due to diffraction. To obtain stable beam shaping results, it is recommended that the distance between the  $F\text{-}\pi\text{Shaper}$  and the focusing lens be in the range 20 - 500 mm.

*Variation of the input beam size results in a variation of output intensity profile!*

Thanks to the features of the optical design, each  $F\text{-}\pi\text{Shaper}$  model is able to work in a wide range of input beam diameters. An increase in the input beam diameter leads to an increase in the intensity of concentric rings in the "Airy disk" pattern, to an increase in the modulation of the intensity distribution and to appearing diffraction side-lobes in a focused spot. Therefore, at a late stage of the adjustment procedure, it is recommended to tune the input beam diameter to ensure the optimal spot profile with minimized side-lobes.

*Variation of the input beam profile results in an intensity profile variation at the  $F\text{-}\pi\text{Shaper}$  output and in a focused spot!*

To ensure an optimum distribution of the output intensity, it is necessary to adapt the size of the input beam.

*The effect of changing the profile of the output beam by changing the size of the input beam can be used to compensate for the deviation of the profile of the input beam from the ideal Gaussian!*

*Note: To evaluate the intensity distribution when working with  $F\text{-}\pi\text{Shaper}$ , it is highly recommended to use dedicated instruments, for example, camera-based beam profilers!*

*Do not use the Scanning Slit beam profilers!*

## 5. Focusing of the Output Beam

The *F- $\pi$ Shaper* output beam is to be focused using a lens or other optical system. When approaching the focal plane of this lens, the size and profile of the beam change, and various spots, such as a flat-top, donut, or “inverse-Gauss”, appear near the lens focus. The features of this transformation, as well as examples of the intensity distributions at focused spots, are described in this chapter as well as in the paper in Appendix 2.

*Note: To analyse the final spots of several tens of microns, it is recommended to use beam profiling instruments dedicated for focused laser beams, like Focus Monitor.*

*Do not use the Scanning Slit beam profilers!*

### 5.1. Requirements to Focusing optics

Any types of focusing optics can be applied: *F- $\theta$*  lenses, microscope objectives, telecentric systems, reflective and catadioptric optics, complex optical systems including beam-expanders, scanners, etc. Since the *F- $\pi$ Shaper* optimizes the interference conditions in the area near the focus, it is very important that the focusing optical system be diffraction limited and not introduce any aberrations disturbing the wave front; for details, see chapter “*Evaluation of focusing or imaging quality*” of the Appendix I.

To evaluate the optical quality of the lens, it is recommended to carry out a simple experiment: focus a TEM<sub>00</sub> laser beam with the lens without any beam shaper and measure the spot size at the waist of the focused beam using a beam profiler or by processing a thin layer material. The spot diameter should be close to the theoretical value calculated by the formula

$$2\omega = \frac{4 \cdot \lambda \cdot F}{\pi \cdot D} \cdot M^2$$

where  $2\omega$  is the spot diameter at  $1/e^2$  intensity,  $\mu\text{m}$ ;  $\lambda$  is the laser wavelength,  $\mu\text{m}$ ;  $D$  is the  $1/e^2$  beam diameter at the lens entrance, mm;  $F$  is the focal length of the lens, mm;  $M^2$  is the beam quality factor. As a rule, the deviation of experimental value from theoretical shouldn't exceed 15-25%.

*Note: If the final spot diameter is several times larger than the theoretical value, then the realization of the necessary beam shaping effect is questionable!*

To align the *F- $\pi$ Shaper*, as well as to better learn the principle of its operation, it is recommended to start working with a lens of 1 meter focal length. Then the laser spot has a size of several hundred microns, the depth of field is several tens of mm; evidently, these conditions are very comfortable for using a camera-based beam profiler to measure irradiance distributions. This makes it possible to analyse the beam profile behaviour when the beam propagates in space by moving the beam profiler along the optical axis in an area close to the focal plane of this 1-meter lens, see Appendix 1 where the “Recommended alignment procedure” for one type of *F- $\pi$ Shaper* is presented.

## 5.2. Theoretical spot profiles

*F-πShaper* optimizes the interference conditions when focusing the light; therefore, a focused beam approaching the focus of the lens experiences a specific transformation of the irradiance distribution, which differs from the Gaussian beam; and this difference in profile behaviour is most pronounced in the beam caustic around the waist:

- when focusing the TEM<sub>00</sub> laser beam, the mathematical description of the profile is constant, - just the Gaussian function, but the beam size changes and has a minimum at the waist, approximately coinciding with the lens focus,
- in the case of focusing the beam using the *F-πShaper*, Fig. 3,
  - o both profile and size are variable,
  - o the beam waist is shifted from focus towards the lens at a double Rayleigh length  $z_R$ ,
  - o the flat-top profile is created in the focus of the lens and in several planes closer to the lens, the so-called “Small flat-top” and “Big flat-top”,
  - o wavefronts in the focal plane (flat-top in focus) and in the “Small flat-top” are flat,
  - o the Donut spot is located between the “Small flat-top” and “Big flat-top”,
  - o all the mentioned profiles exist simultaneously, and the choice of a specific spot is carried out by shifting the working plane along the optical axis,
  - o as shown in Fig. 6, the caustic has a stepwise change in the diameter of the beam,
  - o as a rule, it is recommended to use profiles closer to the lens, as shown in Fig. 3; post-focus profiles of a diverging beam are usually not interesting because of energy dissipation and diffraction effects,
  - o the dimensions of characteristic spots and distances between them are given in Fig. 3:
    - the  $1/e^2$  waist diameter is the same as in the case of a focused Gaussian beam,  $2\omega = d$ ,
    - the FWHM diameter of the flat-top spot in the focal plane is the same as the  $1/e^2$  waist diameter  $d$ ,

*Note: characteristic spot sizes are: the  $1/e^2$  diameter for a Gaussian profile and a FWHM for flat-top!*

- the FWHM diameter of the „Small flat-top“ is 1.3 times larger than the spot in the focal plane,
- the FWHM diameter of the „Big flat-top“ is  $1.7d$ ,
- the FWHM diameter of the Donut spot is  $1.5d$ .

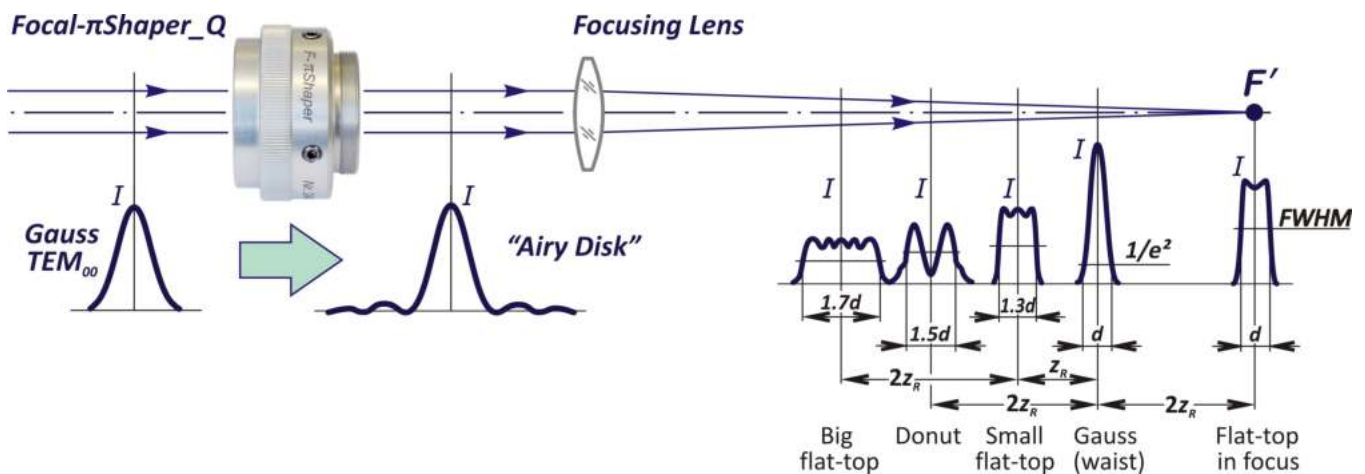


Fig. 3 Transformation of irradiance distribution in an optical system with *F-πShaper*.

Since the principle of operation of the *F-πShaper* involves careful manipulation of the wavefront, the beam integrity is not violated, and the common wavefront is preserved. The spot sizes in the beam caustic are similar to the sizes of focused Gaussian beams; therefore, to determine spot diameters and distances between characteristic planes, well-known formulas can be used to calculate the waist  $1/e^2$  diameter  $d = 2\omega$  and the Rayleigh length  $z_R$  of the TEM<sub>00</sub> beams:

$$z_R = \frac{\pi\omega^2}{\lambda M^2} = \frac{4\lambda M^2}{\pi(2\Theta)^2} = \frac{4\lambda f^2 M^2}{\pi D^2}$$

$$d = 2\omega = \frac{4 \cdot \lambda \cdot F}{\pi \cdot D} \cdot M^2$$

where  $\lambda$  is the laser wavelength,  $D$  is the  $1/e^2$  beam diameter at the lens entrance,  $\Theta$  is the half angle divergence at the  $1/e^2$  irradiance,  $F$  is the focal length of the lens,  $M^2$  is the beam quality factor.

Fig. 2 shows the experimental data on the beam profile transformation and the sequence of characteristic spots, which very well correspond to the theoretical data presented above.

*Variation of the input beam profile results in an intensity profile variation at the F- $\pi$ Shaper output and in a focused spot!*

This effect is demonstrated in Fig. 4, which presents the results of calculations for the “Small flat-top” using optical design software; the conditions for mathematical simulation are as follows:

- Focal- $\pi$ Shaper\_1064\_Q-5;
- the input beam size is variable,  $D = 5 \dots 7$  mm ( $1/e^2$ );
- the working plane “Small flat-top”.

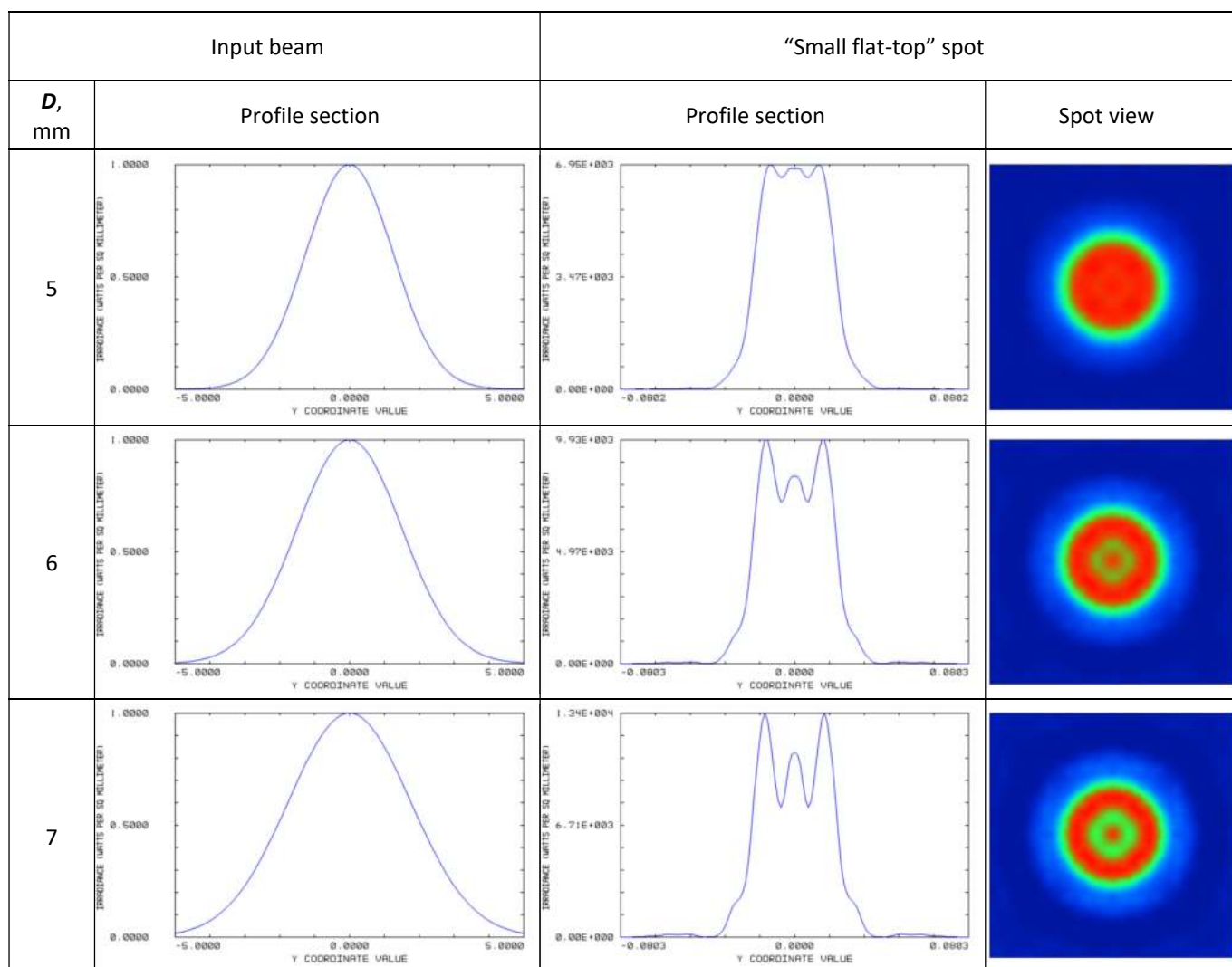


Fig. 4 Change of resulting spot profile by variation of the input beam diameter.

An increase in the input beam diameter leads to stronger modulation of the resulting spot profile; a smoother irradiance distribution is achieved with a reduced input beam size. The optimal profile depends on the requirements of the particular application; most often it can be determined experimentally.

Indeed, in practice, the choice of the optimum input beam diameter also depends on the irradiance distribution of a real laser, which typically deviates from the perfect Gaussian profile.

*The effect of changing the profile of the output beam by changing the size of the input beam can be used to compensate for the deviation of the profile of the input beam from the ideal Gaussian!*

*Note: To evaluate the intensity distribution when working with F- $\pi$ Shaper, it is highly recommended to use dedicated instruments, for example, camera-based beam profilers!*

*Do not use the Scanning Slit beam profilers!*



The results of calculations using optical design software for various diameters of the input beam in various working planes are presented in Fig. 5. Conditions:

- Focal- $\pi$ Shaper\_NUV\_Q-5,
- 2 cases of the input beam  $1/e^2$  diameter:
  - o  $D = 6.6$  mm,
  - o  $D = 5$  mm,
- $\lambda = 532$  nm,
- $M^2 = 1$ ;
- Focusing by diffraction limited lens of 80mm focal length.

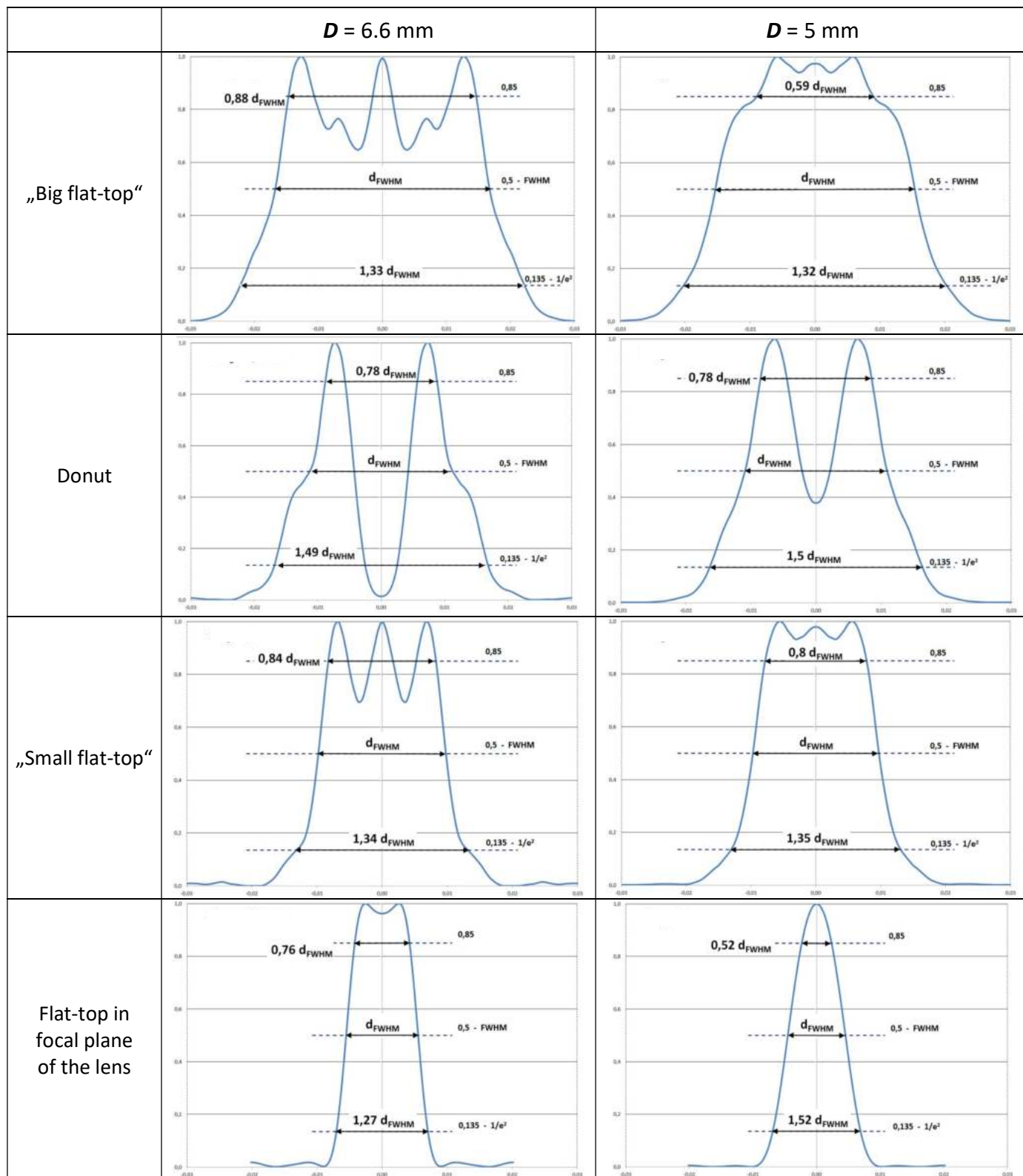


Fig. 5 Change of resulting spot profile by variation of the input beam size.



### 5.3. Experimental spot profiles

Fig. 2 shows an example of beam profile transformation and the sequence of characteristic spots.

Fig. 6 presents the transformation of the spot profiles measured in the caustic of the focused beam after the  $F-\pi$ Shaper in form of combined profiles in different sections along the optical axis. The profiles in individual planes were obtained by a camera-based beam profiler and combined using specialized software. The caustic area with spot types “Big flat-top”, “Donut” and “Small flat-top” is shown on an enlarged scale in the bottom of Fig. 6. Some conclusions about profile transformation in a beam caustic:

- good correspondence between experimental data and theoretical calculations presented in section 5.2,
- when approaching the lens focus, a stepwise change in the total beam size occurs simultaneously with a change in the irradiance profile, - this behaviour is definitely different from the Gaussian beams and is an interesting and important for practice feature of  $F-\pi$ Shaper.

Figs. 7 and 8 show complete sets of measured profiles for different sizes of the input beam, as well as their comparison with the theoretical ones.

Fig. 9 demonstrates theoretical and experimental profiles with increased input beam to generate “Central Peak + Ring”.

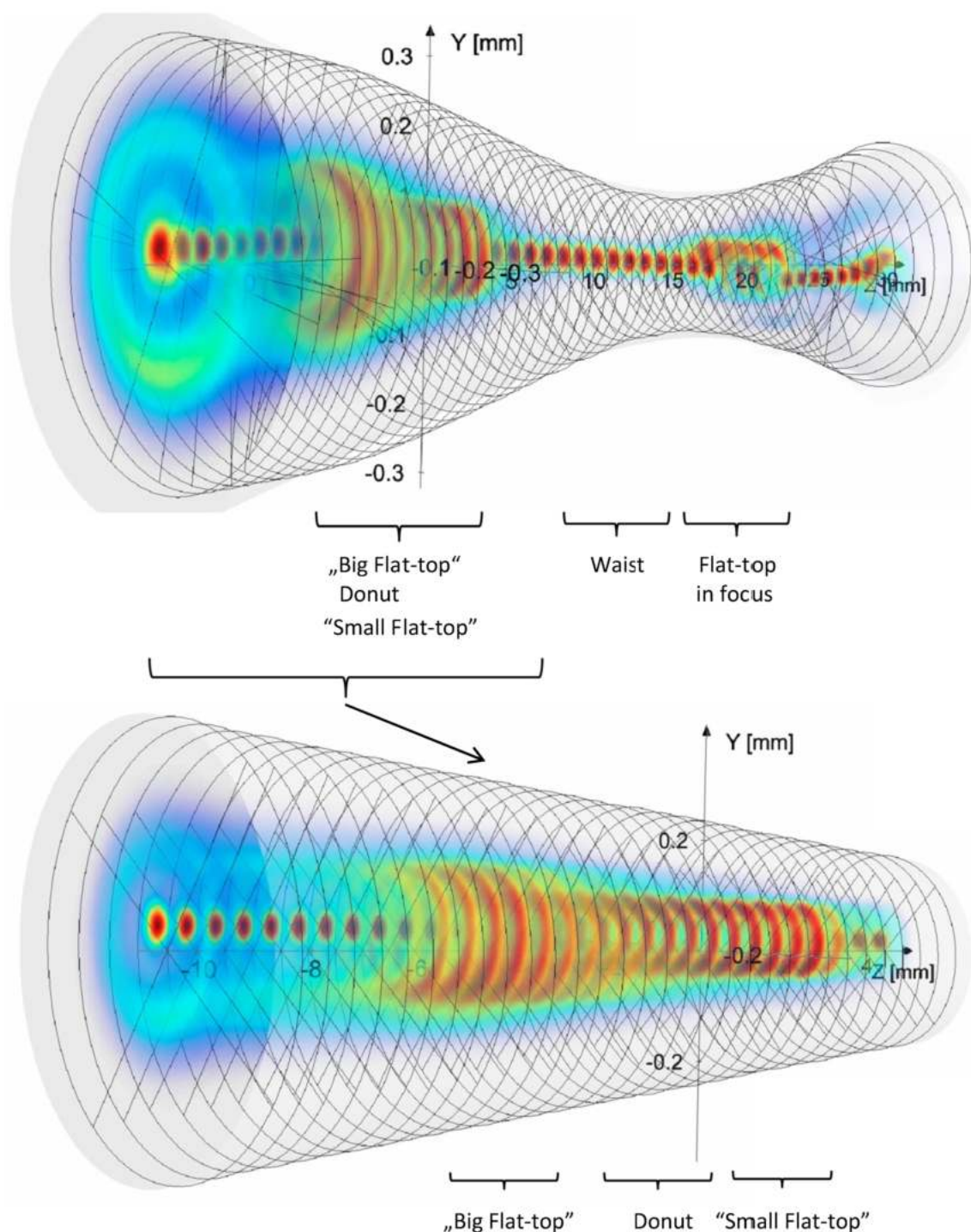


Fig. 6 The spot profile transformation in the caustic of a focused beam in an optical system with  $F-\pi$ Shaper.

### Focal- $\pi$ Shaper\_1064\_Q-5

#### Profile measurements

**Conditions:**

- $D_{\text{Input}} = 5.4 \text{ mm}$  ( $1/e^2$ ),
- Laser: 1064 nm, TEM<sub>00</sub>, fiber coupled,
- Focal- $\pi$ Shaper\_1064\_Q-5,
- Lens of focal length  $\sim 940 \text{ mm}$ ,
- Reference white ring of  $\varnothing 500 \mu\text{m}$ .

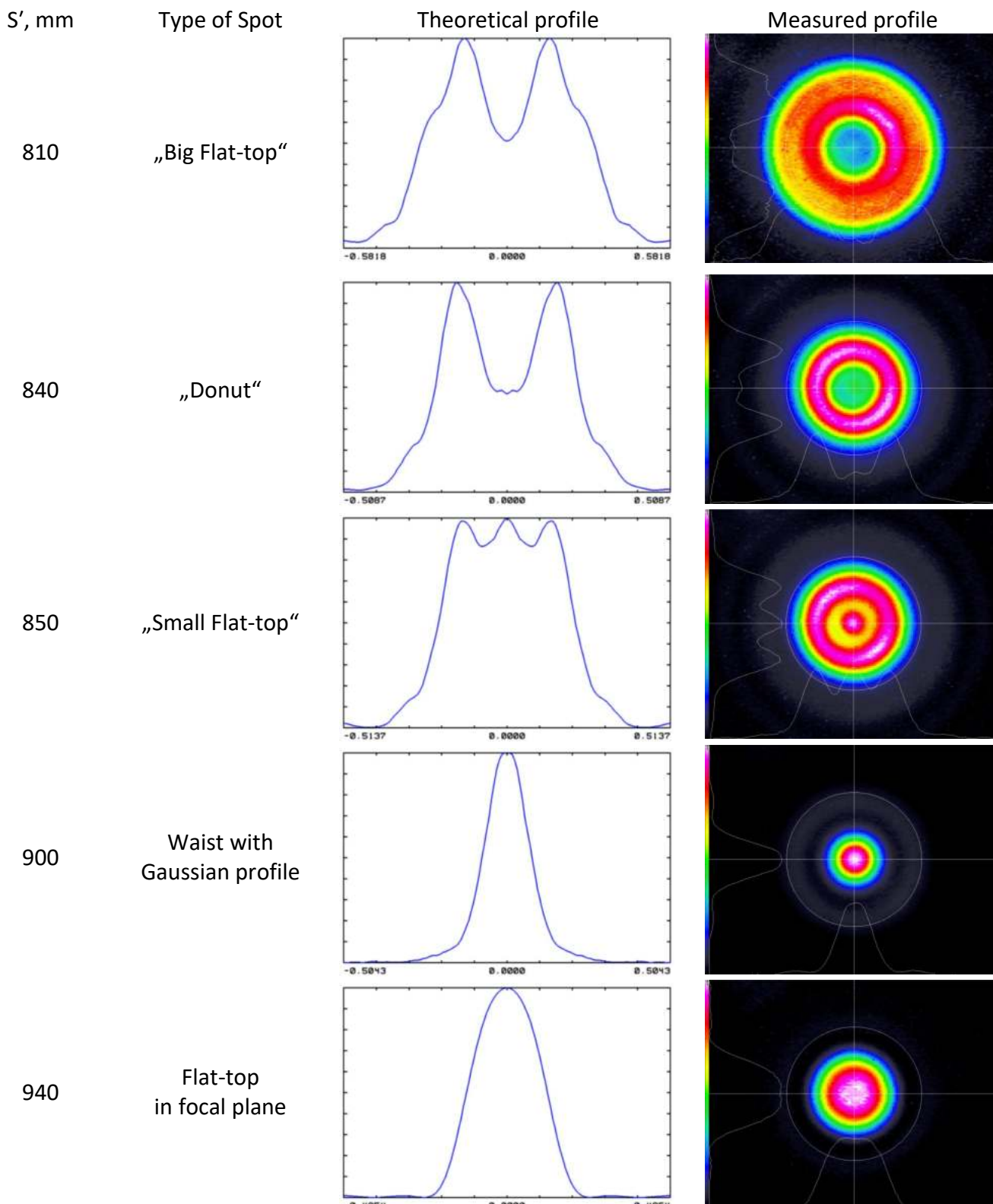
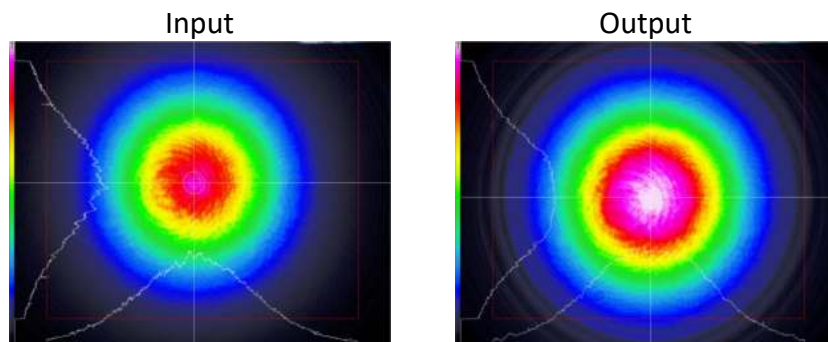
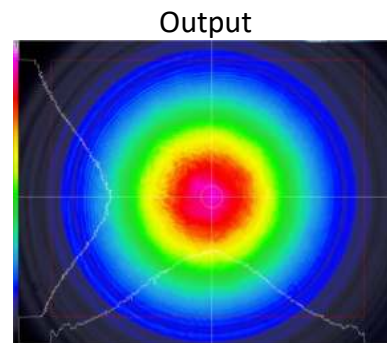
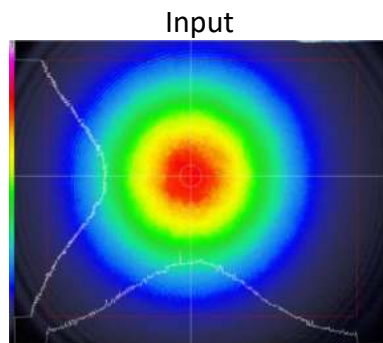


Fig. 7 Profiles for Focal- $\pi$ Shaper\_1064\_Q-5 with  $D_{\text{Input}} = 5.4 \text{ mm}$

**Focal- $\pi$ Shaper\_1064\_Q-5**  
**Profile measurements**

**Conditions:**

- $D_{Input} = 6.4 \text{ mm}$  ( $1/e^2$ ),
- Laser: 1064 nm, TEM<sub>00</sub>, fiber coupled,
- Focal- $\pi$ Shaper\_1064\_Q-5,
- Lens of focal length  $\sim 940 \text{ mm}$ ,
- Reference white ring of  $\varnothing 500 \mu\text{m}$ .

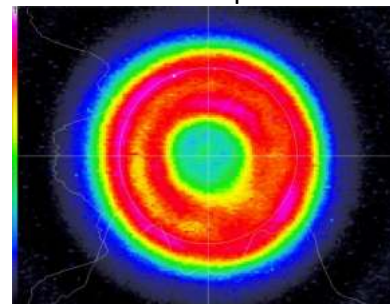
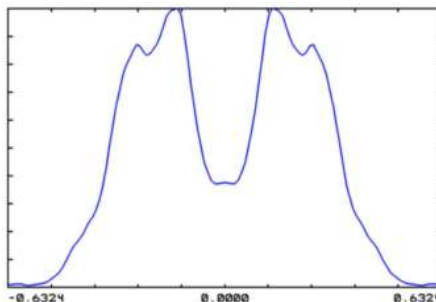


$S'$ , mm      Type of Spot

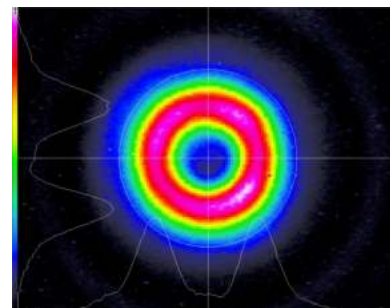
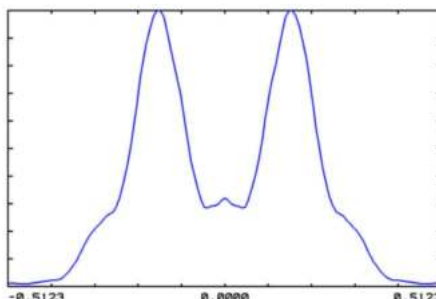
Theoretical profile

Measured profile

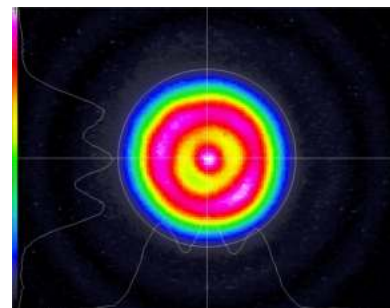
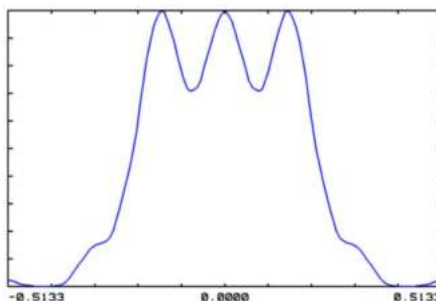
810      „Big Flat-top“



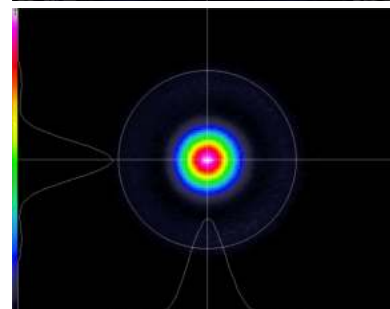
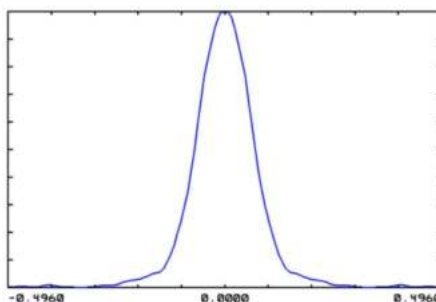
840      „Donut“



850      „Small Flat-top“



900      Waist with Gaussian profile



940      Flat-top in focal plane

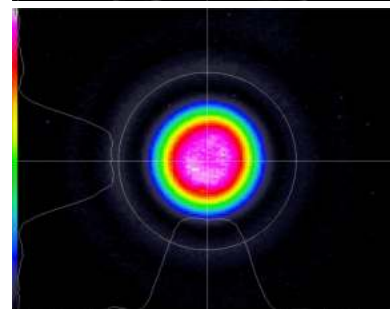
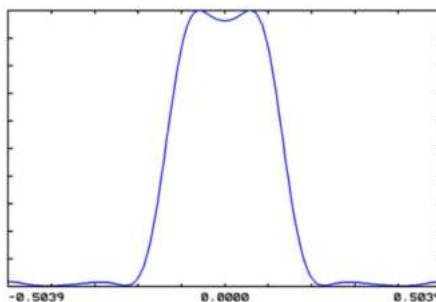


Fig. 8 Profiles for Focal- $\pi$ Shaper\_1064\_Q-5 with  $D_{Input} = 6.4 \text{ mm}$

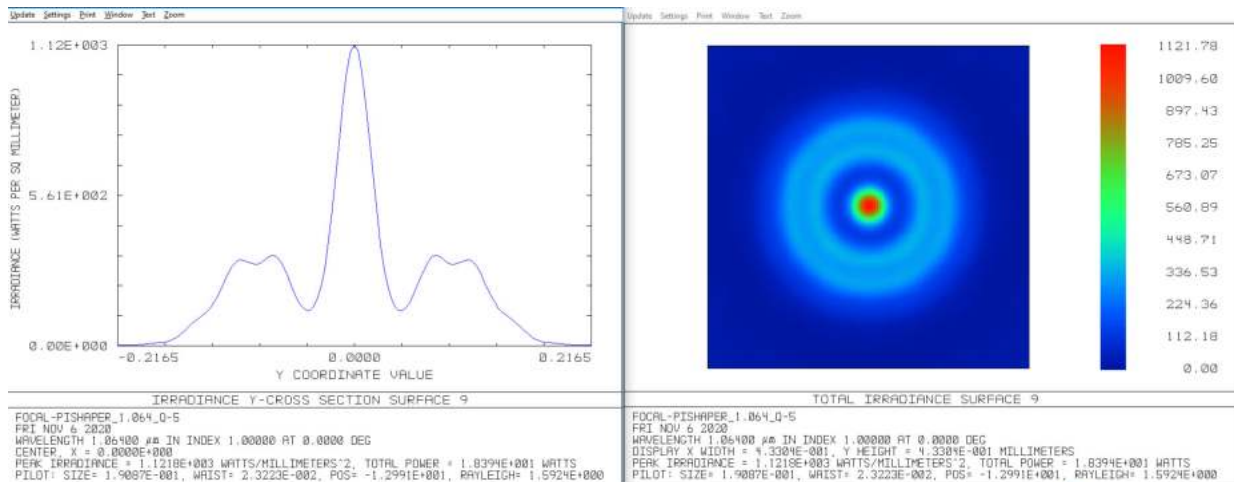


**“Central Peak + Ring” spot**

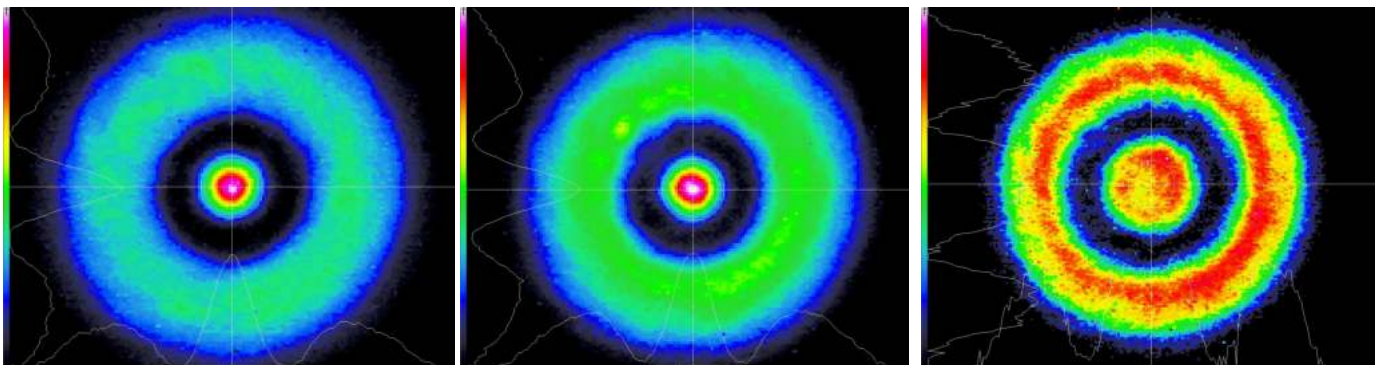
Improvement of industrial laser technologies, for example reduction of spatter in welding aluminium (Al) and copper (Cu) workpieces using IR lasers or 3D-printing (LPBF, Cladding), can be achieved by optimizing temperature distribution in the working zone using a specific spot “Central Peak + Ring” – high intensity central peak surrounded by a ring of lower or even intensity. This specific spot can be realized by applying TEM<sub>00</sub> laser beam of larger diameter compared to the diameter specified for a particular *F-πShaper* model, this approach is illustrated in Fig.9 for *Focal-πShaper\_NUV\_Q-3*, input beam  $D_{Input} = 6.3 \text{ mm}$  ( $1/e^2$ ),  $\lambda = 520 \text{ nm}$ :

- (a) - theoretical profile section and spot view in the plane between the “Big Flat-top” and the “Donut”,
- (b), (c) - measured profiles in planes along the optical axis in zone between the “Big Flat-top” and the “Donut”,
- (d) - measured profile in the plane of “Big Flat-top” spot,
- (e) - measured profile in the plane between the “Small Flat-top” and the beam Waist,
- (f) - measured profile in the plane of “Small Flat-top” spot.

In summary, increasing input beam size and de-focusing the workpiece makes it possible to control intensity distribution in the working zone and reaching optimal temperature distribution.



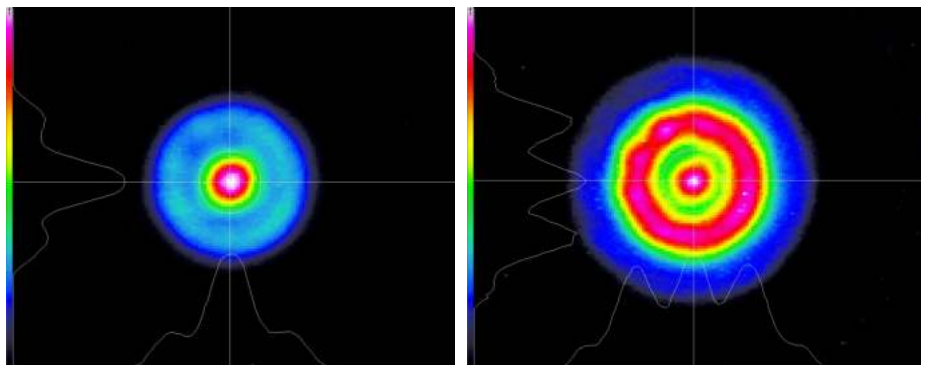
(a)



(b)

(c)

(d)



(e)

(f)

Fig. 9 Creating “Central Peak + Ring” spot with Focal-πShaper\_NUV\_Q-3 by  $D_{Input} = 6.3 \text{ mm}$ ,  $\lambda = 520 \text{ nm}$

## 6. Spectral Properties

The optical components of the *F- $\pi$ Shaper* are made of fused silica, sapphire, these materials are characterized by low dispersion, the optical design is optimized for operation in a specific working band, and the AR-coating of each *F- $\pi$ Shaper* model is optimized for the respective spectrum, detailed specifications are given in Table 2.

Table 2

Focal- $\pi$ Shaper model	AR-coating	Optimum* spectrum, nm	Working band, nm (acceptable performance)	Material of lenses
_1064_Q	V-type @1064 nm	1020 - 1100	920 - 1200	Fused Silica
_1070_Q_HP	V-type @1070 nm	1020 - 1100	920 - 1200	Sapphire
_NIR_Q	Broadband	1500 - 2100	1400 - 2200	Fused Silica
_TiS_Q	V-type @800 nm	750 - 900	720 - 1050	Fused Silica
_NUV_Q	Broadband	335 - 560	310 - 580	Fused Silica
_266_Q	V-type @266 nm	250 - 275	240 - 290	Fused Silica
_CO2_Q	V-type @10000 nm	9400 - 10600	9000 - 11000	ZnSe

Spectral transmission graphs for the popular *F- $\pi$ Shaper* models are presented in Fig. 10. These data are based on measurements of reflection of the optical surfaces with AR-coatings. Units manufactured in various production batches may have deviations from the presented graphs.

When operating in the Optimum spectrum, the total losses do not exceed 2%.

Most of the *F- $\pi$ Shaper* models, developed for use in relatively narrow spectral band, have V-type AR-coatings with minima at the design wavelengths, Table 1, are applied.

The *F- $\pi$ Shaper\_NUV\_Q* models have broad band AR-coatings optimized for the working spectral band.

Using *F- $\pi$ Shaper* at a wavelength outside the optimal spectral band will affect the increasing in loss.

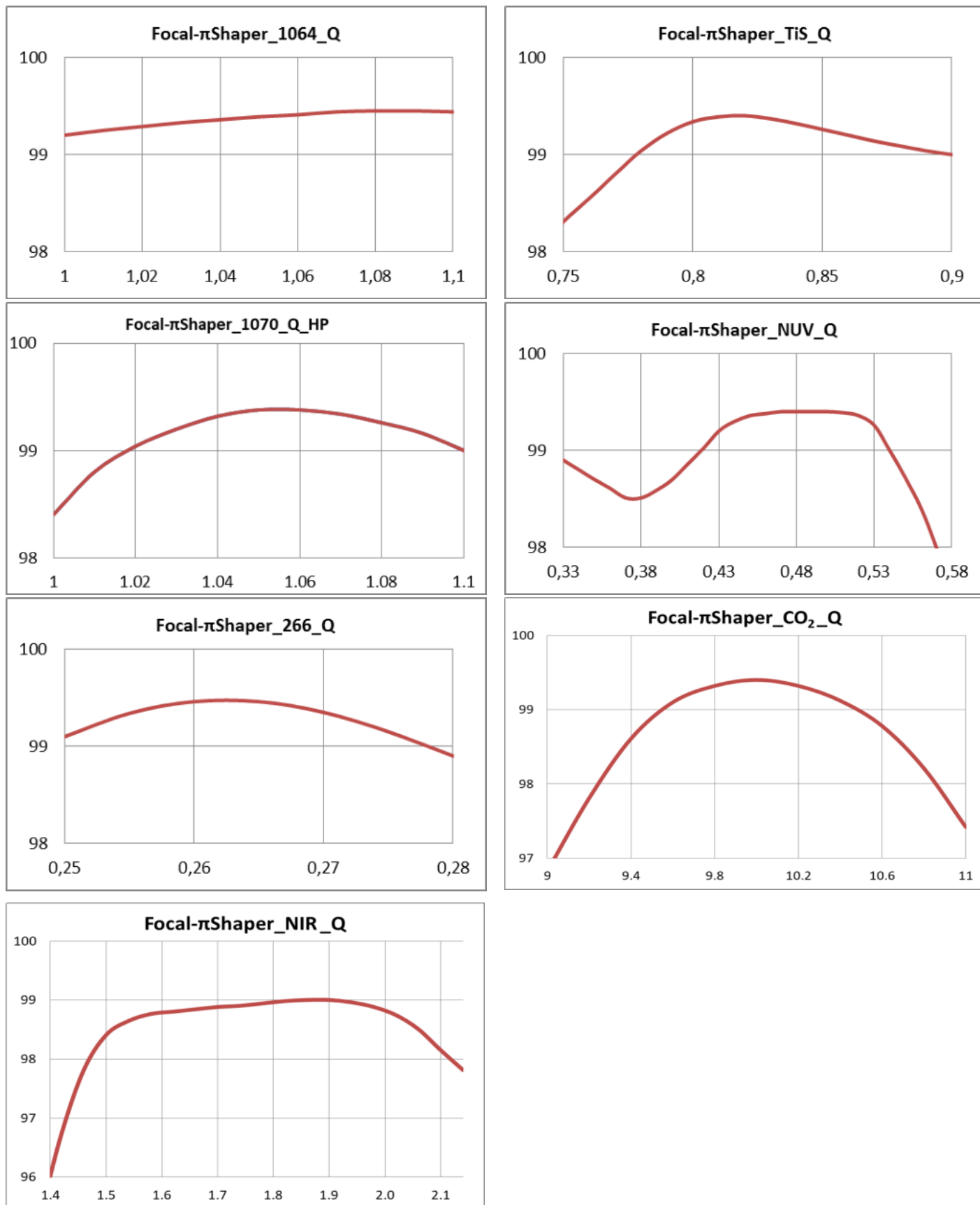


Figure 10 *F\_πShaper* Spectral transmission, %, versus wavelength, μm, other explanations in text.

## 7. Features of design and operation

Outlook and general drawings of the *F- $\pi$ Shaper* are presented in Fig. 11 and 12. There are 2 basic designs:

- with CA 20 mm and mounting outer/inner threads M30x0.75, Fig. 11,
- with CA 38 mm and mounting outer/inner threads M58x1, Fig. 12.

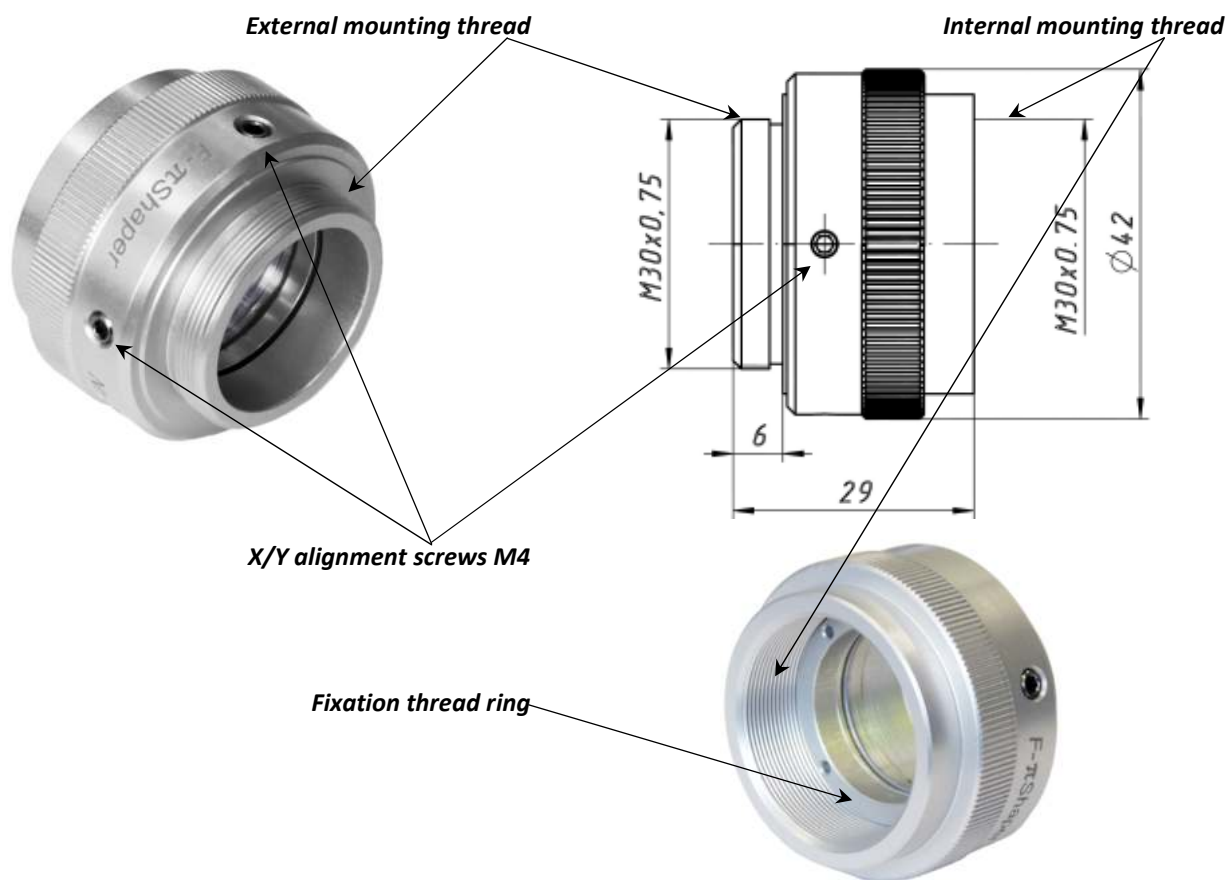


Fig. 11 *F- $\pi$ Shaper* with CA 20 mm and outer/inner mounting threads M30x0.75.

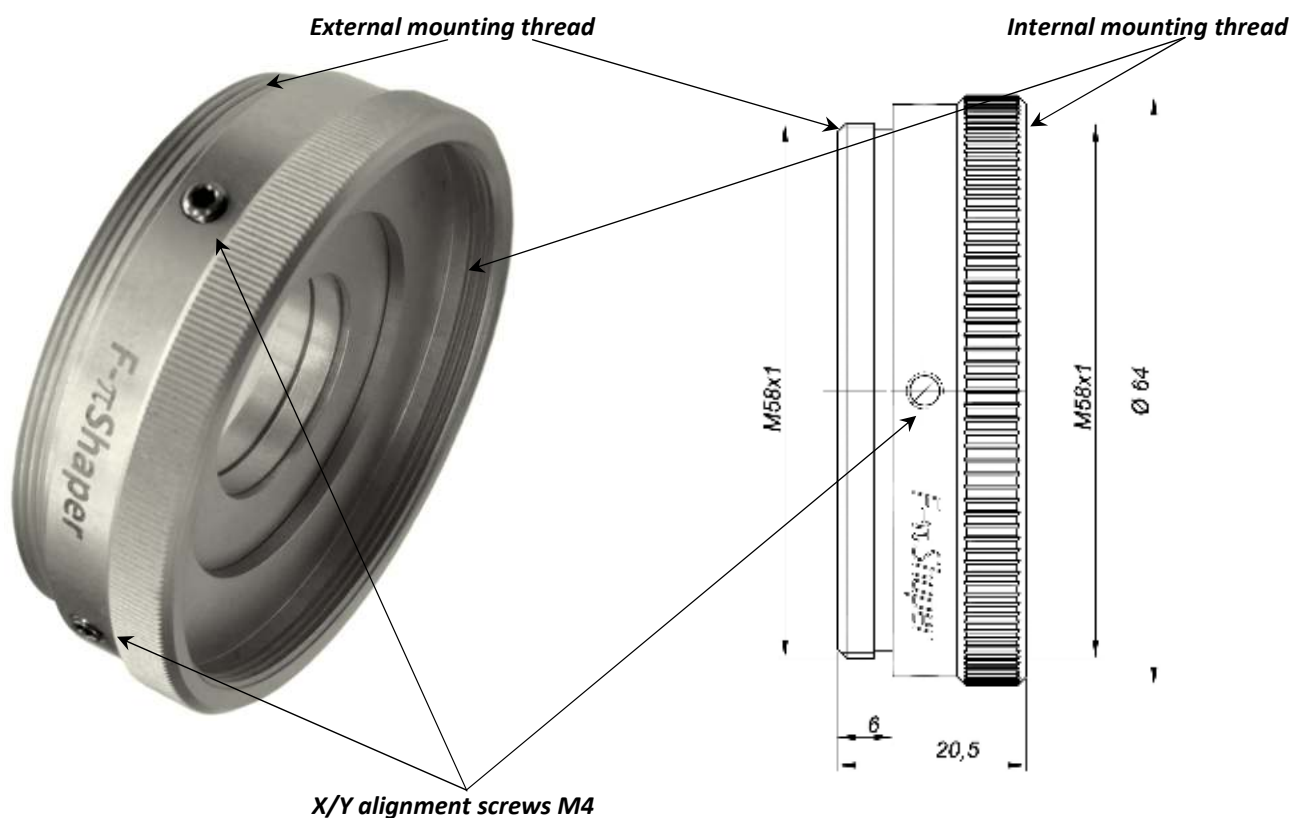


Fig. 12 *F- $\pi$ Shaper* with CA 38 mm and outer/inner mounting threads M58x1.



### Mounting in equipment

The mounting threads are compatible with the widely used in industry collimators Optoskand and similar ones, to simplify the integration of the *F- $\pi$ Shaper* into customer equipment without auxiliary adapters. Nevertheless, if adaptors are required, the models presented in Fig. 12 are available.

*F- $\pi$ Shaper* devices are equipped with internal tools for X/Y alignment:

- four ball-end thrust screws for lateral translation,
- adjustment range  $\pm 2$  mm,
- the recommended alignment procedure includes step-by-step loosening and strengthening of the screws, with the control of the intensity profile of the output beam,
- the criterion for proper alignment is the symmetric pattern of the circular fringes at the *F- $\pi$ Shaper* output, see the examples in Figs. 7 and 8, top right.

*Note: To evaluate the intensity distribution when working with F- $\pi$ Shaper, it is highly recommended to use dedicated instruments, for example, camera-based beam profilers!*

*Do not use the Scanning Slit beam profilers!*

It is assumed that the *F- $\pi$ Shaper* will be mounted in the optical system using the intended threads and adapters; other installation methods should be discussed with the supplier

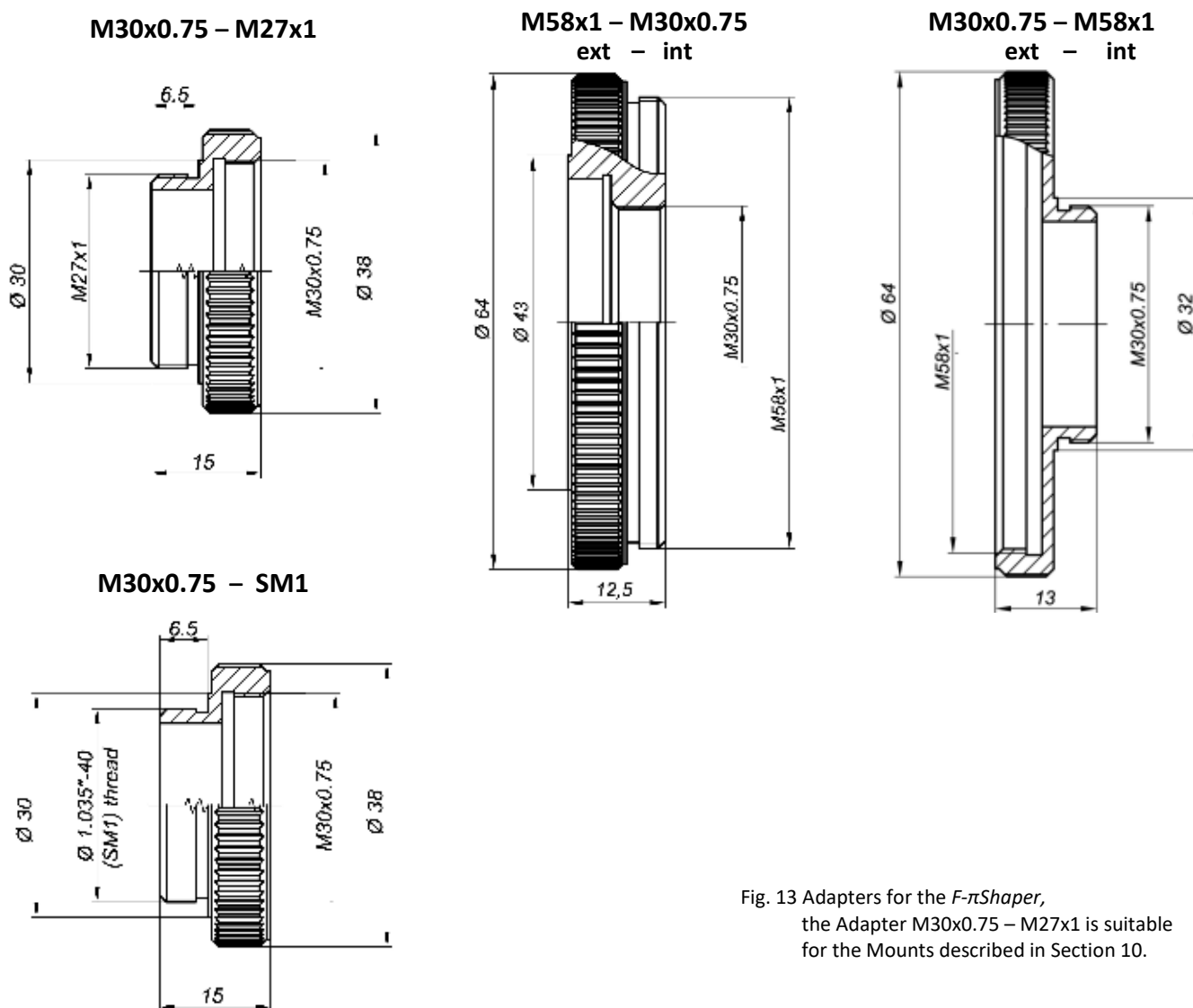


Fig. 13 Adapters for the *F- $\pi$ Shaper*, the Adapter M30x0.75 – M27x1 is suitable for the Mounts described in Section 10.

## 8. Location of $F-\pi$ Shaper in equipment

$F-\pi$ Shaper should normally be located

- after the collimator or beam expander, that is, after optical devices optimizing the input beam diameter, Fig.15 (a), (b),
- in front of the diffraction limited focusing optics or the scanning optical system including a focusing lens such as  $F-\theta$  lens.
- installing a beam expander after a  $F-\pi$ Shaper is possible and recommended when optimizing input beam for a scanner is required in a particular laser technology, Fig.15 (c).

Since  $F-\pi$ Shaper are afocal optical systems with  $\sim 1^x$  magnification, the divergence angle and the size of the output beam remain the same as at the  $F-\pi$ Shaper input. Therefore, there is no problem using any mirror-based scanners, such as galvo-mirror scanning heads or polygon scanners.

**Important:** *No clipping or truncating the laser beam is allowed in the optical system before or after the  $F-\pi$ Shaper! The operation physical principle presumes that the whole focused beam creates the resulting flat-top spot. Clipping disturbs the interference effect, leads to destroy of the resulting spot profile and diffraction side-lobes.*

The structure of the output profile remains stable over long distances, usually more than 1 meter. To obtain stable beam shaping results, it is recommended that the distance between the  $F-\pi$ Shaper and the focusing lens be in the range of 20 - 500 mm and, when chosen, be fixed while the equipment is in operation. If the processing head in the laser equipment is movable, the  $F-\pi$ Shaper must be mounted on this head to maintain a constant distance to the focusing lens.

If required in a specific application, one can apply a beam expander after the  $F-\pi$ Shaper, but before the scanning head. Such an approach may be reasonable, for example, when a smaller or variable size of the resulting spot is required.

An example of a typical implementation of an optical system with  $F-\pi$ Shaper in laser equipment for Selective Laser Melting technology (3D-printing) is shown in Fig. 14.

Other recommended layouts with  $F-\pi$ Shaper are shown in Fig. 15.

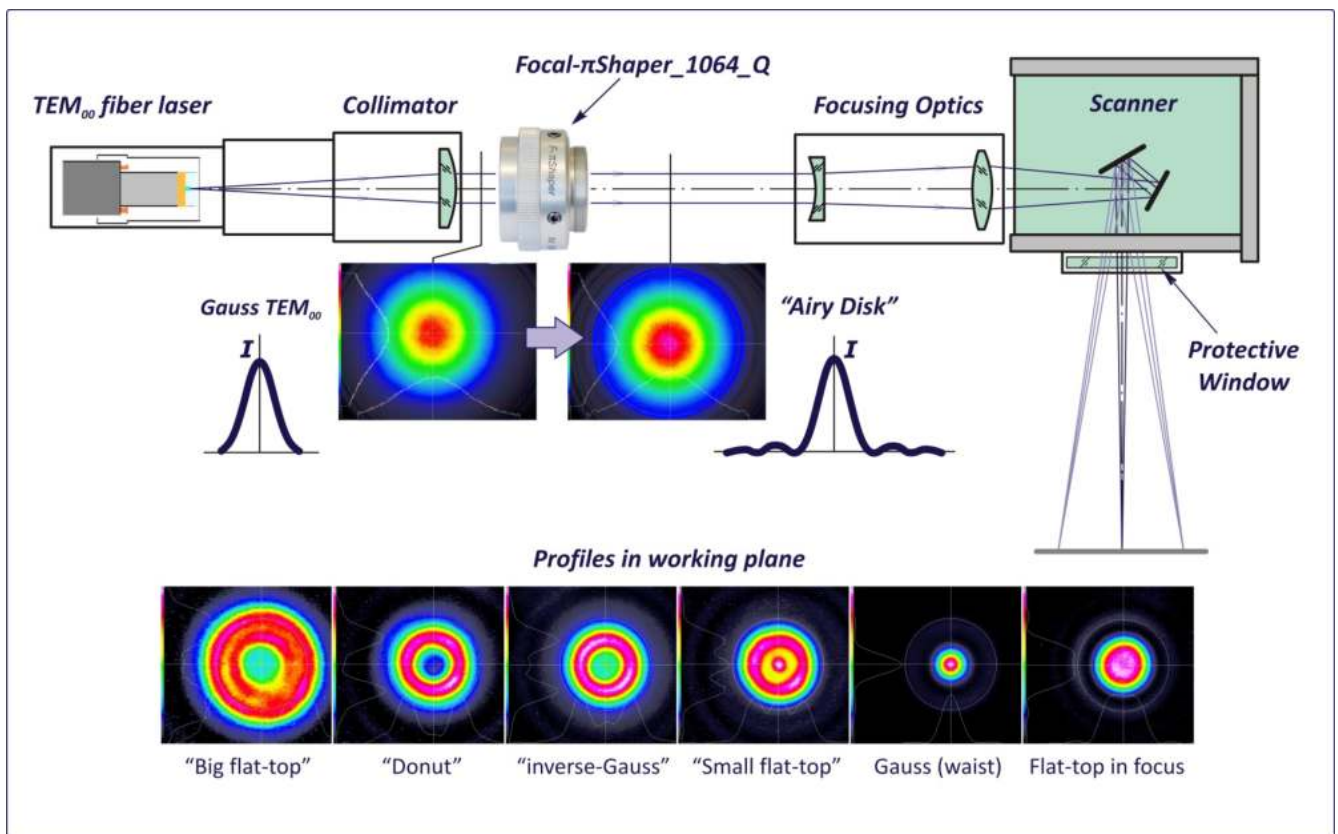


Fig. 14 An example of the positioning of the  $F-\pi$ Shaper in laser equipment for Laser Powder Bed Fusion (L-PBF).

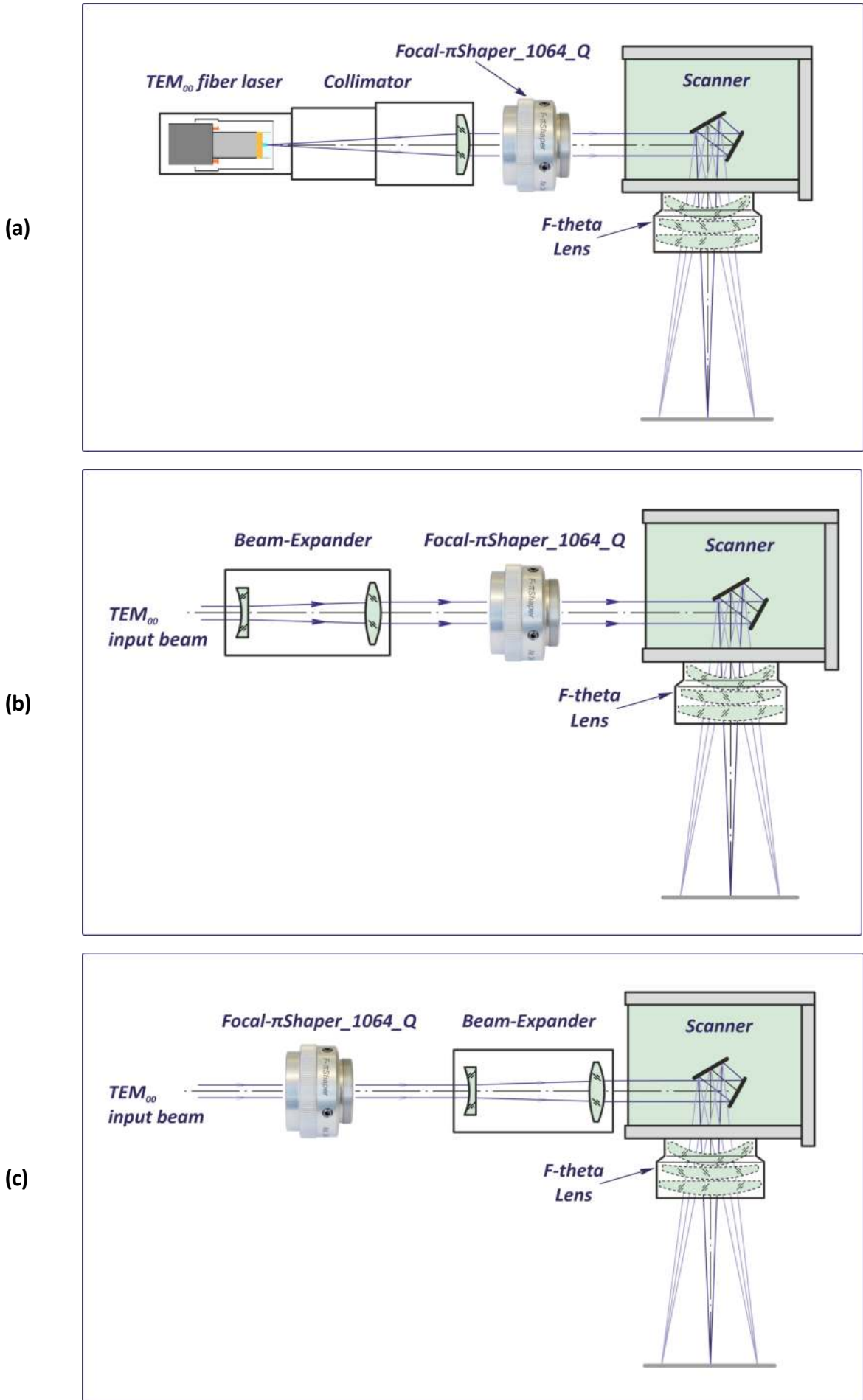


Fig. 15 Various layouts of the positioning of the *F- $\pi$ Shaper* in laser equipment .

## 9. Example of using *F-πShaper* in equipment for Laser Powder Bed Fusion (L-PBF)

L-PBF machine with the optical system described in Fig. 14, was used for processing in various conditions:

- various intensity distributions,
- various protective windows.

Fig. 16 presents a comparison of the views of processing areas during the recording process using the Gaussian and Donut laser spots, the measured spot profiles and traces when processing a steel plate are shown in the bottom of the figure.

Summarizing the features of the processes with different spot profiles, one can state that switching from the “Gaussian” to the “Donut” spot allows optimizing technological processes:

- less sparking,
- less porosity of the workpiece,
- more efficient use of laser energy, which improves productivity,
- higher stability and reliability of the process results during long-term operation.

Photos in Fig. 17 demonstrate a part manufactured of metal powder using L-PBF equipment with an optimized optical system comprising the *Focal-πShaper* and the *aThermoXX* protective windows. Characteristic features are:

- about 17 cm in diameter,
- smooth outer surfaces,
- low porosity, which is very important in ultra-high vacuum applications.

The data presented confirm the feasibility of building optical systems for L-PBF equipment with the control of thermal effects in the melting pool and in the optical system using the *Focal-πShaper*, which creates a “Donut” spot, and the *aThermoXX* protective windows, minimizing the thermally induced focus shift and aberrations.

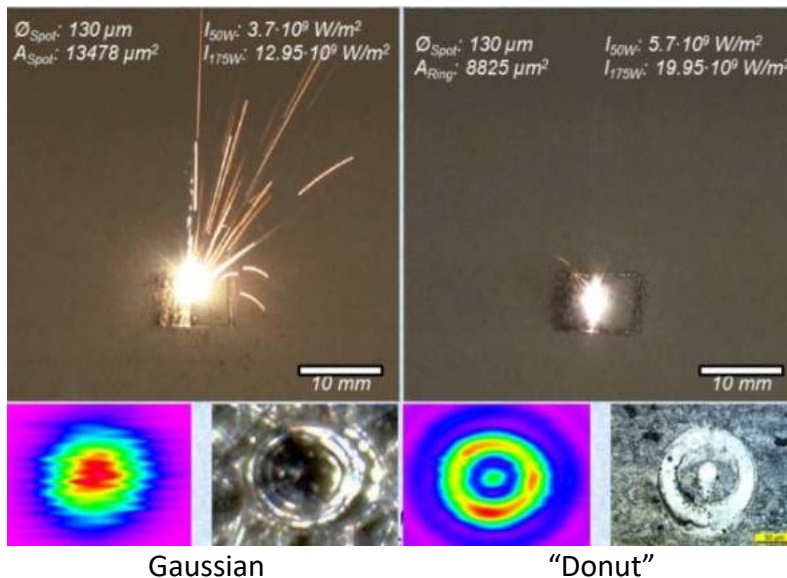


Fig. 16 Comparison of sparking during processing using Gaussian and Donut spots.

(Courtesy of Forschungszentrum Jülich)

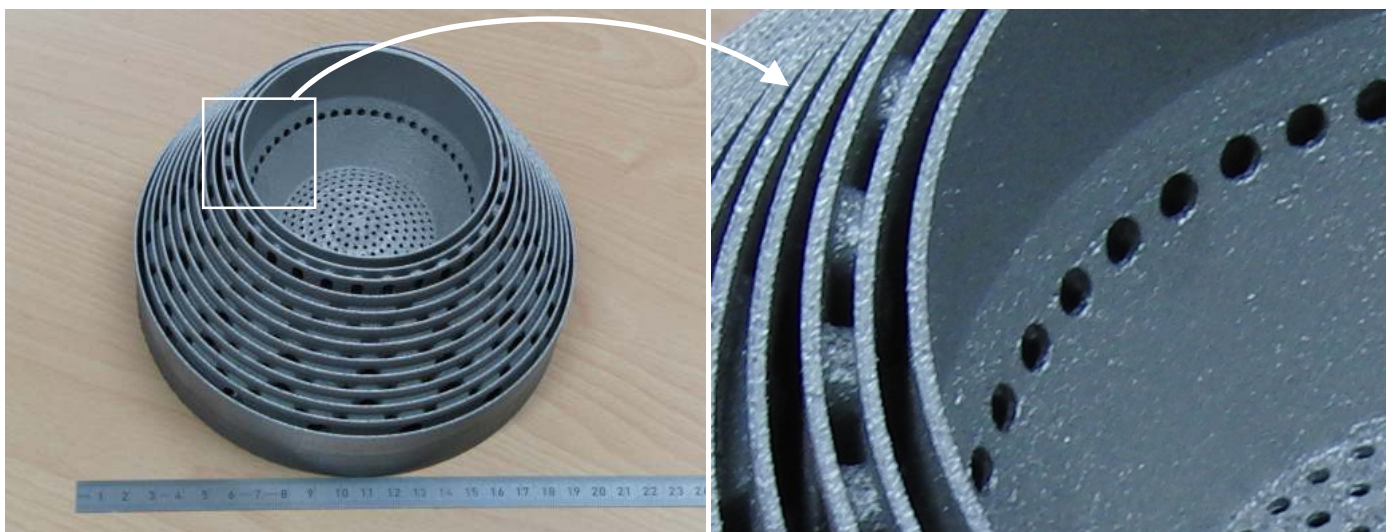


Fig. 17 Example of the manufactured part (Courtesy of Forschungszentrum Jülich).



## 10. Alignment

*Focal- $\pi$ Shaper\_Q* is an optical system capable to operate in a relatively wide angular field of view up to  $5^\circ$  and in a wide range of divergence angles of the input beam,  $\pm 20$  mrad; therefore, it is insensitive to tilt errors (angular misalignments) with respect to the input beam when mounted in the optical system of laser equipment. However, the *F- $\pi$ Shaper* requires proper X/Y lateral alignment to ensure a symmetric pattern of the circular fringes of the output beam; examples of output profiles with the correct X/Y alignment are presented in Figs. 7 and 8, top right.

*F- $\pi$ Shaper* is equipped with internal tools for X/Y alignment, Figs. 11 and 12:

- four ball-end thrust screws for lateral translation,
- adjustment range  $\pm 2$  mm,
- the recommended alignment procedure includes step-by-step loosening and strengthening of the screws, with the control of the intensity profile of the output beam,
- the criterion for proper alignment is the symmetric pattern of the circular fringes at the *F- $\pi$ Shaper* output, see the examples in Figs. 7 and 8, top right.

*Notes:* To evaluate the intensity distribution when working with *F- $\pi$ Shaper*, it is highly recommended to use dedicated instruments, for example, camera-based beam profilers!

To analyze the final spots of several tens of microns, it is recommended to use beam profiling instruments dedicated for focused laser beams, like Focus Monitor

*Do not use the Scanning Slit beam profilers!*

At the alignment stage, it is recommended to provide an input beam of maximum diameter, and then the beam shaping effect will be most pronounced, which simplifies the alignment process and makes it more reliable. At a late stage of the adjustment procedure, it is necessary to tune the input beam diameter to ensure the optimum profile with minimized side-lobes in the working spot.

The recommended alignment procedure is presented in Appendix.

If, when mounting the *F- $\pi$ Shaper* in laser equipment, a wider range of X/Y lateral alignment is required, then it can be extended with an external mount; for example, a lockable Mount M27 or a 4-axis Mount (without locking) presented in Figs. 18 and 19.

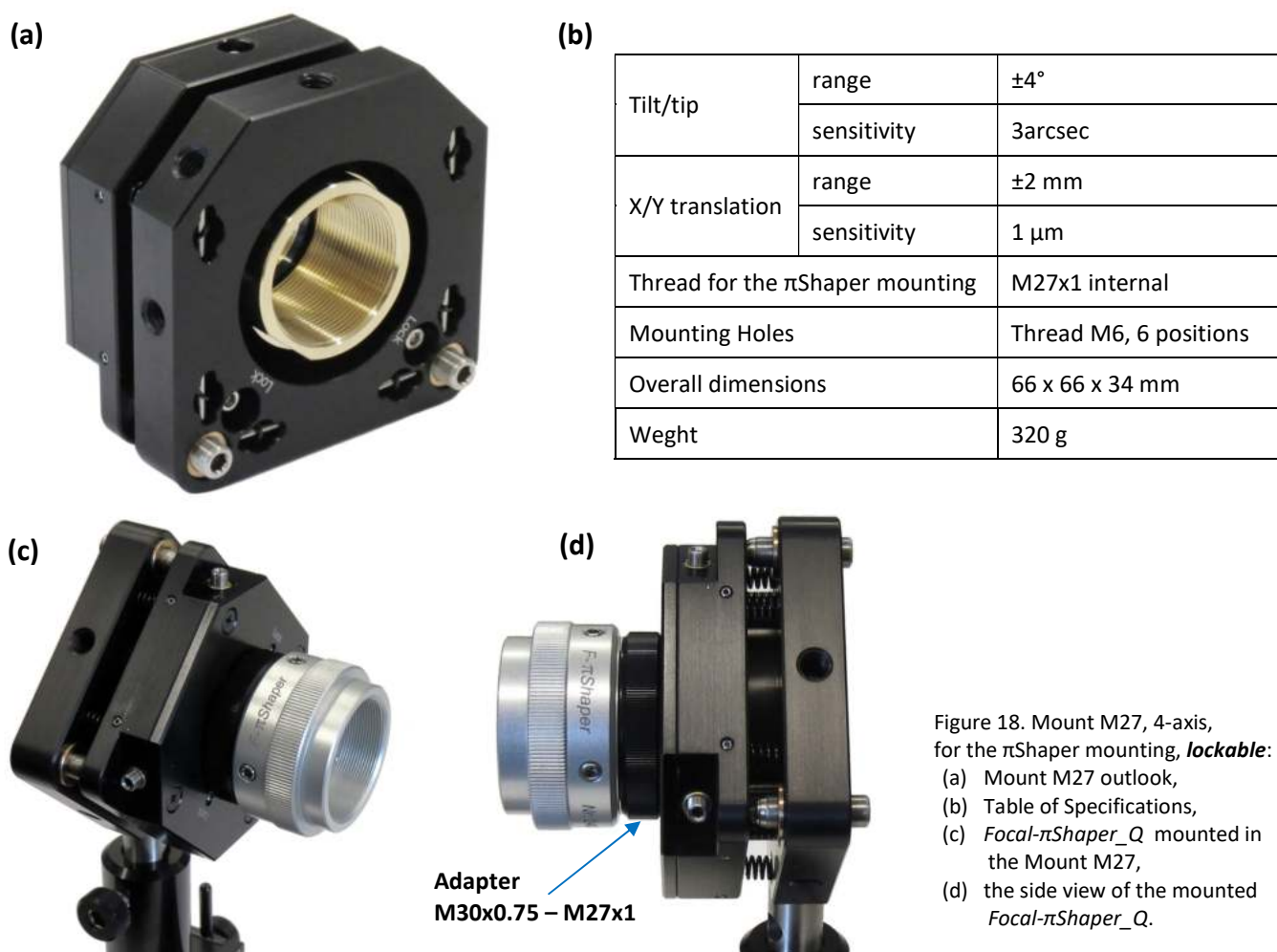


Figure 18. Mount M27, 4-axis, for the  $\pi$ Shaper mounting, **lockable**:  
 (a) Mount M27 outlook,  
 (b) Table of Specifications,  
 (c) *Focal- $\pi$ Shaper\_Q* mounted in the Mount M27,  
 (d) the side view of the mounted *Focal- $\pi$ Shaper\_Q*.

The lockable 4-axis Mount M27, Fig. 18, provides firm alignment and fixation of the  $F-\pi$ Shaper, it is recommended for use in industrial equipment, as well as in other applications where stable positioning of the optics is required. Examples of mounting the  $F-\pi$ Shaper using the Mount M27 with a demonstration of design features are presented in Fig. 18 (c),(d).

Detailed design information about the Mount M27 is presented in [http://pishaper.com/shaper\\_adjust.html#tabs-1](http://pishaper.com/shaper_adjust.html#tabs-1)

The 4-axis Mount presented in Fig. 19 is not equipped with locks; however, it has the knurled screws, which makes it very convenient for use in laboratory conditions or for quick setup of the  $\pi$ Shaper for test purposes, see also

[http://pishaper.com/shaper\\_adjust.html#tabs-2](http://pishaper.com/shaper_adjust.html#tabs-2)

Tilt/tip	ange	$\pm 2^\circ$
	sensitivity	3 arcsec
X/Y translation	range	$\pm 2$ mm
	sensitivity	1 $\mu$ m
Thread for the $\pi$ Shaper mounting		M27x1 internal
Mounting Hole		Thread M6, 2 positions
Overall dimensions		77 x 77 65 mm
Weight		200 g



Figure 19. 4-axis Mount, without locking, for laboratory use.

The *symmetrical* view of the beam profile pattern at the  $F-\pi$ Shaper output is a criterion for proper alignment.

*Note: To evaluate the intensity distribution when working with  $F-\pi$ Shaper, it is highly recommended to use dedicated instruments, for example, camera-based beam profilers!*

*Do not use the Scanning Slit beam profilers!*

The lateral displacement tolerance of the  $F-\pi$ Shaper is  $\pm 0,1$  mm.

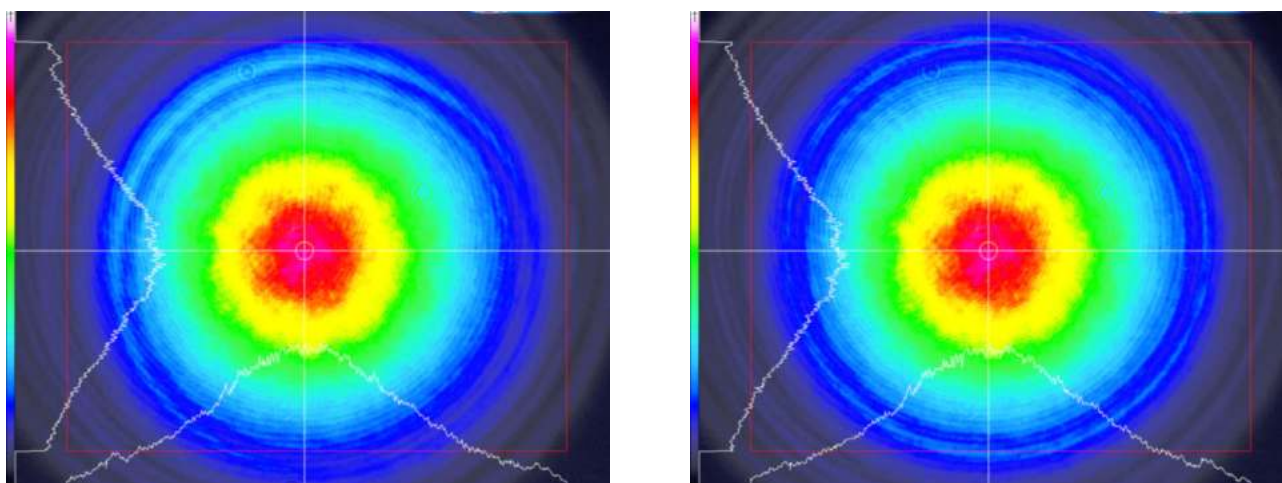
Examples of the beam profile transformation, when the correct  $\pi$ Shaper alignment, are presented in Figs. 2, 7, 8.

Recommendations to alignment procedure are presented also in section 11.2 and in

[http://www.adloptica.com/manual/Alignment\\_pish66\\_f\\_pish9.pdf](http://www.adloptica.com/manual/Alignment_pish66_f_pish9.pdf)

<http://youtu.be/hinnppo4knY>

<http://pishaper.com/pdfs/alignment.zip?Align=Download+Alignment+video>



Misaligned

Correct alignment

Fig. 20 Examples of output beam profiles with the  $F-\pi$ Shaper:

left – misaligned, vertical and horizontal lateral displacements, right – when correct alignment

## 11. APPENDIX

### 11.1. Evaluation of focusing or imaging quality

Usually, at the initial stage of analysing the optics performance, evaluation of focusability is considered for the case of perfect focusing or imaging, i.e. when only diffraction causes the focus spot broadening and determines the physical resolution.

However, real optical systems have aberrations, and real scientific and engineering practice requires development of criteria for evaluating focusing or imaging quality. There are several resolution criteria to specify the quality of an optical system or construction tolerances; choice of the appropriate criterion depends on the particular task or application. Most used in technical optics [1,2] criteria are:

- *Point Spread Function (PSF)* describes irradiance distribution in the focal or image plane owing to diffraction in presence of geometrical aberrations,
- *Optical Transfer Function (OTF)* is the Fourier transform of the PSF, the modulus of the OTF is called the *Modulation Transfer Function (MTF)* and represents the contrast of a sinusoidal periodic structure in the image; these functions present basic specifications of imaging quality for optics in photography and other imaging applications; this topic is out of scope of this publication, but is discussed in details in the specialized literature [1],
- *Strehl ratio* is defined as the ratio of the maximum irradiance of the aberrated diffraction PSF to that under the perfect imaging or focusing conditions, this is a complex characteristic of the optical system,
- *Rayleigh limit*, postulating that the diffraction image remains practically unchanged, that is, limited by diffraction, when geometrical aberrations are negligible and the maximum wavefront aberration  $w_{max}$  (deviation of a wavefront from the perfect sphere) is less than approximately  $\lambda/4$ ,
- *Maréchal criterion*, establishing that the image is diffraction limited when the root-mean-square (RMS) wavefront aberration  $w_{RMS}$  doesn't exceeds  $\lambda/14$ .

Note, the Rayleigh limit is not the same as the *Rayleigh criterion* introduced to resolve the separate spots. The Rayleigh limit is useful in considering monotone wavefront aberration functions, however, is not completely valid for oscillating functions. That is why the Maréchal criterion is used as a universal method to characterize the diffraction limited focusing or imaging when geometrical aberrations are negligible and physical resolution is limited by diffraction effects only; it was originally introduced for imaging optics, but is also used for focusing of laser beams. The interrelation of various criteria is summarized in Table 3.3.

In practice of optical designing, it is also convenient to compare the geometrical spot size when presence of aberrations and the Airy disk diameter: *in optics with close to diffraction limited imaging or focusing, the geometrical spot is always inscribed in the Airy disk circle.*

**Interrelation of various criteria to specify the focusing and imaging quality**

Table 3.3

<i>Focusing spot</i>	<i>Maximum wavefront aberration <math>w_{max}</math> (monotone functions)</i>	<i>RMS wavefront aberration <math>w_{RMS}</math></i>	<i>Strehl ratio</i>
Diffraction limited	$< \lambda/4$ Rayleigh limit	$< \lambda/14$ Maréchal criterion	$> 0.8$
Defined by diffraction and aberrations	$\lambda/4 - \lambda/2$	$\lambda/14 - \lambda/6$	0.4 - 0.8
Defined mainly by aberrations	$> \lambda/2$	$> \lambda/6$	$< 0.4$

1. M. Born, E. Wolf, *Principles of Optics*, 6th edn. (Pergamon Press, Oxford, 1980)
2. D. Malacara-Hernández, Z. Malacara-Hernández: *Handbook of Optical Design*, 3rd ed. (CRC Press, Boca Raton, Florida 2013)



**11.2. Recommended alignment procedure for Focal- $\pi$ Shaper\_Q**

**Introduction**

The basic approach of the recommended alignment procedure is as follows:

- implementation of an optical system with *F- $\pi$ Shaper* shown in Figs. 21, 22 (same as Figs. 2, 3),
- the *F- $\pi$ Shaper* and the laser must be located in the equipment in predetermined positions,
- alignment of the *F- $\pi$ Shaper* with respect to the laser,
- removing the normal focusing lens or objective for the alignment purpose,
- use as a Focusing Lens the *Alignment Lens Q* of 1000mm focal length, then the spots in the area of the lens focus will be several hundred microns, which can be detected using commercially available camera-based beam profilers,
- use of a laser at an operating power level; if necessary, use an attenuator to suppress laser power while maintaining the properties of the laser beam, including on-axis astigmatism,
- analysis of beam profiles using dedicated instruments beam profilers:
  - in front of the *F- $\pi$ Shaper*,
  - right after the *F- $\pi$ Shaper*, for example, at a distance in the range of 30-100 mm,
  - Donut and flat-top spots in the area of the lens focus in planes located closer to the “Alignment Lens Q”, that is, in the planes shown in Fig. 21,

*A complete set of test data should include measurements of the entire beam caustic in the area of the lens focus of with finding all the characteristic spots shown in Figs. 21 and 22.*

- achieving circular symmetry of the above mentioned profiles using alignment tools for X/Y lateral translation,
- when the X/Y alignment of the *F- $\pi$ Shaper* with respect to the laser beam is finished, the *Alignment Lens Q* should be replaced with a normal lens of the equipment.

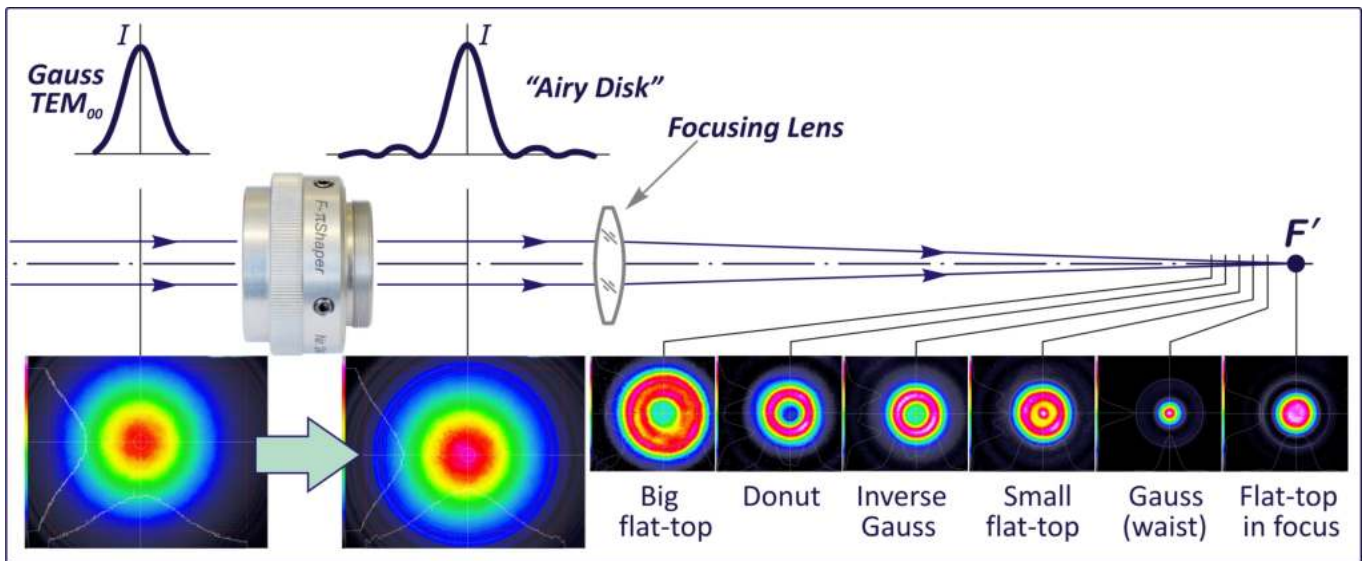


Fig. 21 The principle of operation of the *Focal- $\pi$ Shaper\_Q* with examples of measured profiles.

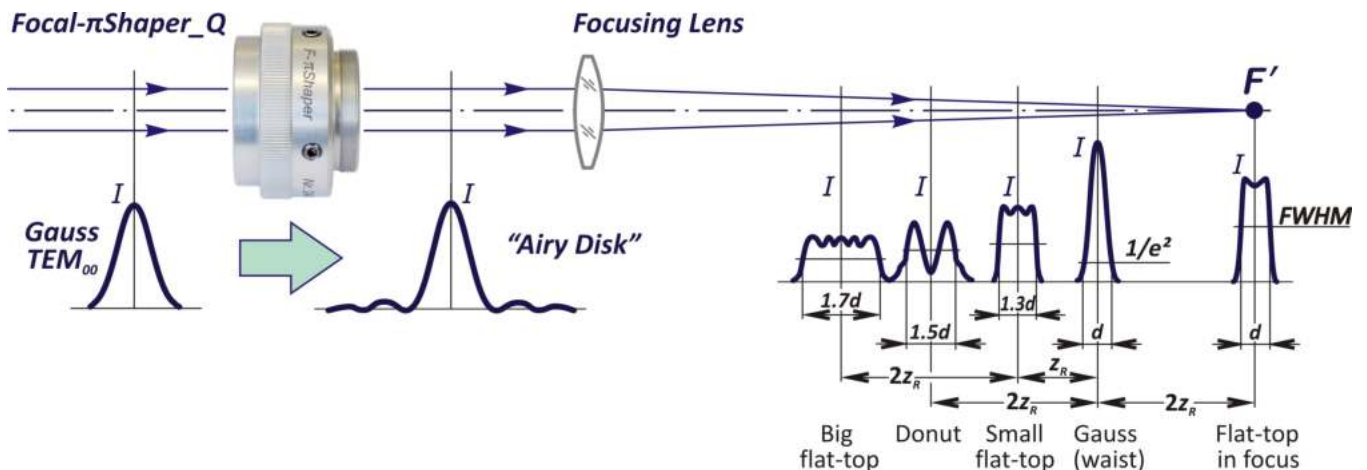


Fig. 22 Transformation of irradiance distribution in an optical system with *F- $\pi$ Shaper*.

Notes: Usually, when installing a beam shaper in certain equipment, it is recommended to align the optical system of this equipment without a beam shaper, and then install the beam shaper and align it with control of measured input and output intensity profiles.

To evaluate the intensity distribution when working with F- $\pi$ Shaper, it is highly recommended to use dedicated instruments, for example, camera-based beam profilers or Focus Monitor!

Do not use the Scanning Slit beam profilers!

The optomechanical elements used in the considered alignment procedure are shown in Figs. 23 and 24.

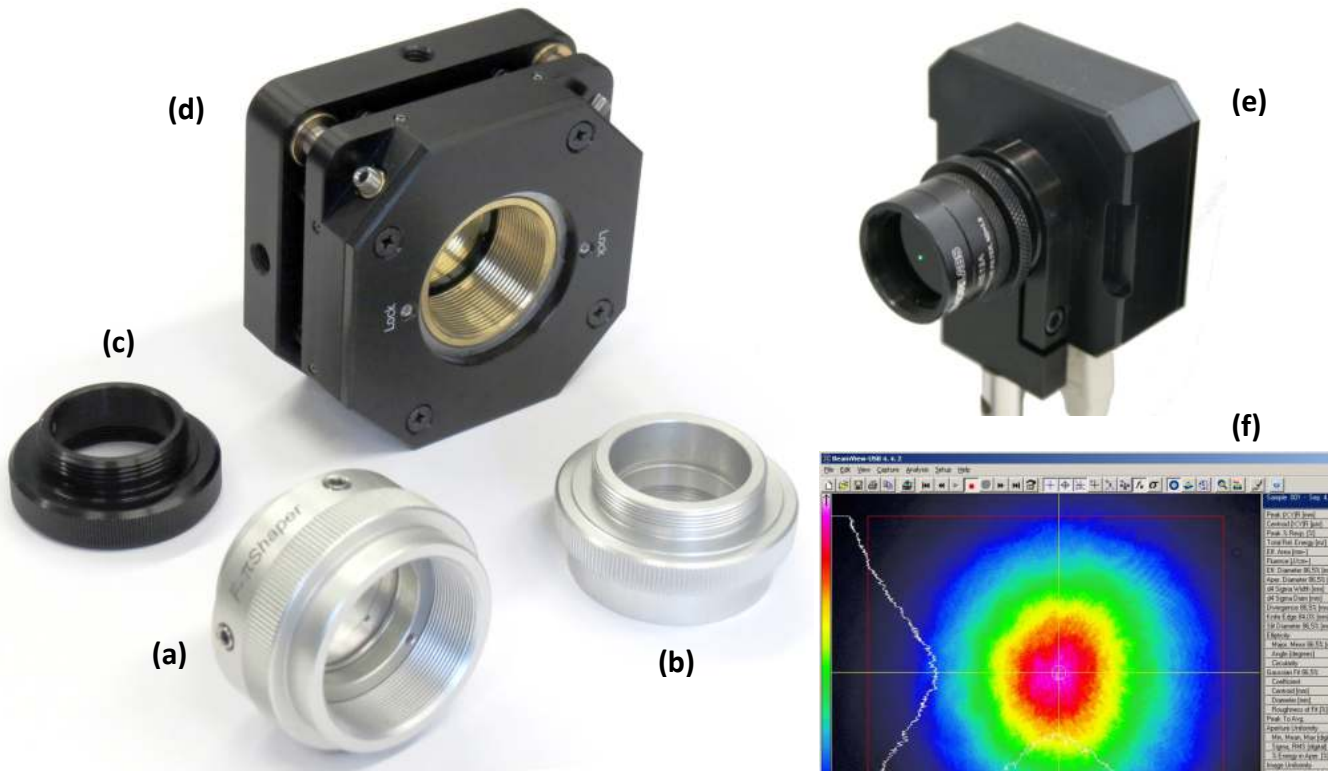


Fig. 23 Optomechanical components used during the alignment procedure of the F- $\pi$ Shaper:  
 (a) F- $\pi$ Shaper, (b) Alignment Lens Q, (c) Adapter M30x0.75 – M27x1, (d) Mount M27, 4-axis,  
 (e) Camera based beam profiler, (f) Screenshot of the measured profile in the software of the beam profiler.

Alignment Lens Q is a lens with a focal length of  $\sim 1000$  mm mounted in a holder compatible with the mounting threads of the F- $\pi$ Shaper, Fig. 24.

The Alignment Lens Q is used for the purposes of alignment **only** !

Alignment Lens Q  
 Alignment Lens Q for UV

Compatible with Focal- $\pi$ Shaper Q  
 Focal length 1000 mm  
 Clear Aperture  $\varnothing 22$  mm

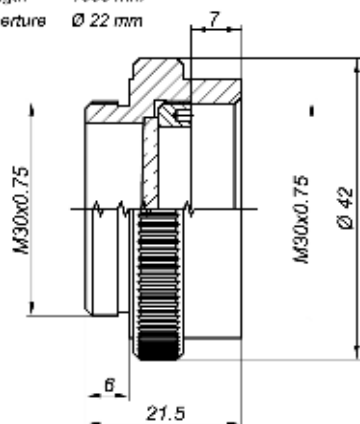


Fig. 24 Alignment Lens Q.

The principle of operation of the *F- $\pi$ Shaper* involves the use of diffraction limited focusing optical system; therefore, the auxiliary lens of 1000 mm focal length, the *Alignment Lens Q*, is a convenient alignment tool:

- it replaces a *Normal working lens* (F- $\Theta$  lens, etc.) for the alignment purpose,
- is free from aberrations for typical laser beam sizes up to 20 mm, therefore, provides the condition of the diffraction limited focusing of light,
- the outer and inner threads M30x0.75 are compatible with the threads on the *F- $\pi$ Shaper*, which simplifies the installation of the *Alignment Lens Q* and the entire alignment procedure,
- due to relatively big focal length, the spots in the area of the lens focus will be several hundred microns, which can be detected and analyzed using modern camera-based beam profilers,
- the Rayleigh length of the focused beam is several tens millimetres, which simplifies the analysis of profiles created in the focus area of the *Alignment Lens Q*,
- when the X/Y alignment of the *F- $\pi$ Shaper* with respect to the laser beam is completed, the *Alignment Lens Q* should be replaced with the *Normal working lens* of the equipment.

When the *F- $\pi$ Shaper* is properly aligned with the laser beam, the transformation of the beam intensity profile with the normal lens of the equipment will be the same as with the *Alignment Lens Q*, but

- the spot diameters will be reduced in proportion to the **ratio** of the focal lengths of the *Normal lens* and the *Alignment Lens Q*,
- reduction of the Rayleigh length, which practically defines the depth of focus (DOF), will be proportional to the **square of the ratio** of the focal lengths of the *Normal lens* and the *Alignment Lens Q*.

For example, when switching from the *Alignment Lens Q* of 1000 mm focal length to the *Normal lens* with the focal length of 100 mm, the spots will be 10 times smaller, while the DOF 100 times (!) narrower.

When the *F- $\pi$ Shaper* is correctly aligned with the laser beam and the *Normal lens* installed in the optical system of the equipment, then the size of the resulting spots are usually less than 100  $\mu\text{m}$ , and measurements using camera-based beam profilers are not reliable. Therefore, it is recommended to test system performance, including alignment, by processing real materials. It is preferable to use materials with a direct correspondence of the processing result to the intensity distribution of a spot; for example, ablation of a thin film on a substrate or direct ablation of material, as shown in Fig 34.

*A complete set of test data should include measurements of the entire beam caustic in the area of the lens focus with the detection of all characteristic spots shown in Figs. 21 and 22.*

During the alignment procedure on the equipment, the beam profiler should be located at a distance of about 1000 mm from the *Alignment Lens Q*. In case of mechanical constrains in the positioning of the beam profiler, it is recommended to use mirrors to bend the optical path and make the alignment setup more compact.

*Important: No clipping or truncating the laser beam is allowed in the optical system before or after the F- $\pi$ Shaper!  
The operation physical principle presumes that the whole focused beam creates the resulting flat-top spot.  
Clipping disturbs the interference effect, leads to destroy of the resulting spot profile and diffraction side-lobes.*

The below description presents stepwise alignment procedure, where each step is illustrated with photos and screenshots from the beam profiler software; the conditions are

- *F- $\pi$ Shaper\_NUV\_Q-5*,
- a laser of  $\lambda = 520 \text{ nm}$ , fiber coupled TEM<sub>00</sub> diode laser,
- a collimated beam with 6.4mm  $1/e^2$  diameter provided by the laser collimator,
- the camera-based beam profiler is used, Fig. 23(e),
- the Mount M27 is used,
- X/Y alignment is performed using four ball-end thrust screws of the *F- $\pi$ Shaper* and the Mount M27.



## Alignment procedure

### 11.2.1. Input beam profile

- install the Laser,
- install the camera-based *Beam Profiler*,
- measure the laser beam profile, see the example of screenshot in Fig. 25, which is the *input beam profile*.

#### Note:

*It is recommended to use an input beam of maximum diameter, and then the beam shaping effect will be more pronounced, which simplifies the alignment process and makes it more reliable.*

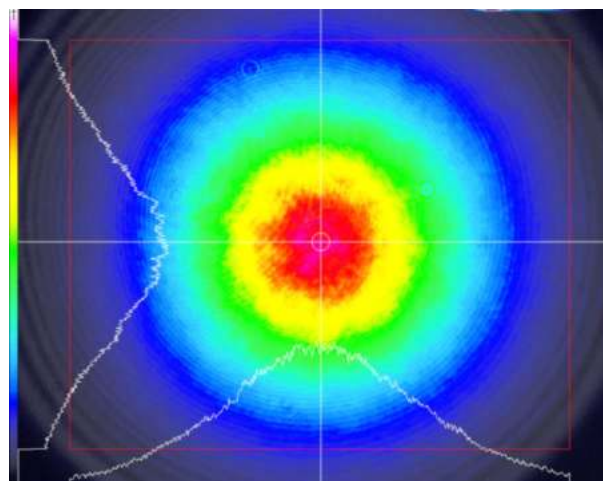


Fig. 25 Screenshot of input beam profile.

### 11.2.2. *F*- $\pi$ Shaper

- install the *F*- $\pi$ Shaper using the *Mount M27* and the *Adapter M30x0.75 – M27x1*,
- example of the mounting is shown in photo, Fig. 26,
- provide approximate centering of the *F*- $\pi$ Shaper with respect to the laser beam so that the range of lateral X/Y translation of the alignment tools is sufficient for further displacement correction.

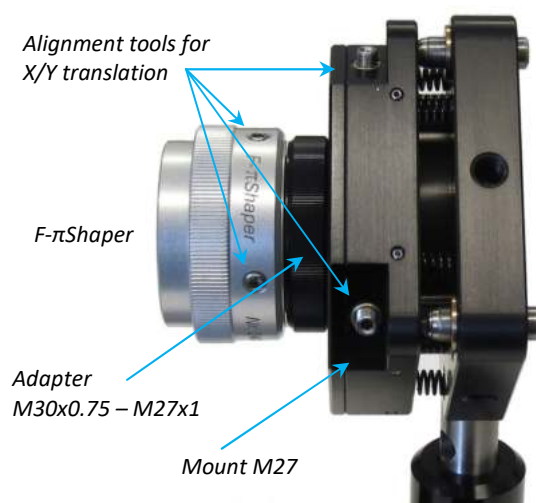


Fig. 26 *F*- $\pi$ Shaper installed in the *Mount M27*.

### 11.2.3. Output beam profile

- install the *Beam Profiler* after the *F*- $\pi$ Shaper,
- measure the *output beam profile*, see examples of screenshots for the misaligned *F*- $\pi$ Shaper in Fig. 27,
- the *output beam profile* is close to the Airy disk function: the bright round Gaussian-like central region is surrounded by a series of concentric rings of relatively low intensity, see also section 4,

*Note: The output beam profile SHOULD NOT be Flat-top !*

- the concentric rings in Fig. 27(a) are displaced horizontally to the right, and in Fig. 27(b) - vertically downwards and horizontally to the right, – these patterns are certain signs of the *F*- $\pi$ Shaper displacements.

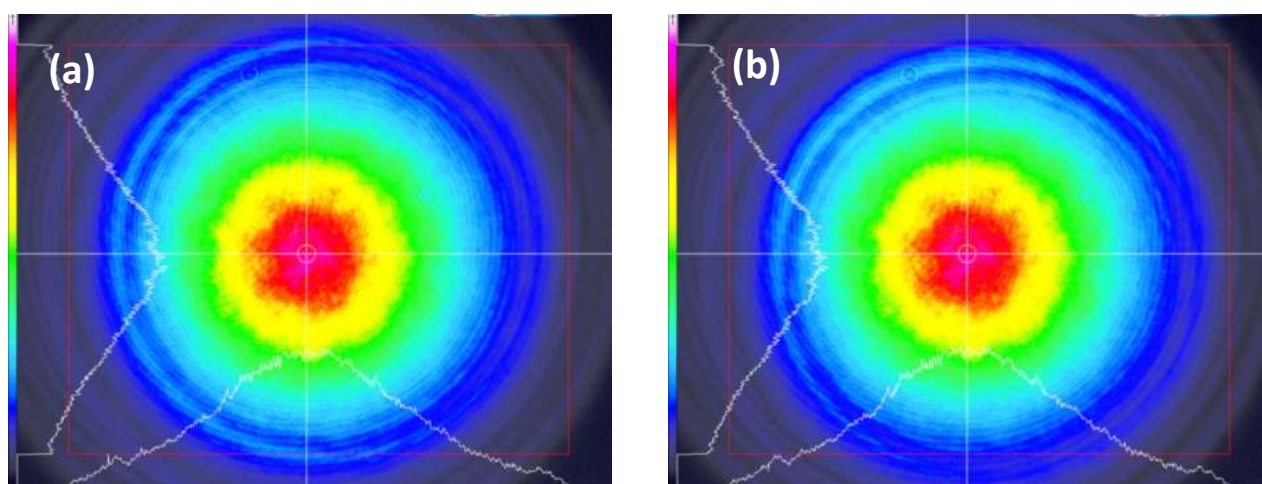


Fig. 27 Output beam profile when misaligned *F*- $\pi$ Shaper:

(a) **horizontal** lateral displacement to the right,

(b) lateral displacements: **vertical** downwards, **horizontal** to the right.

#### 11.2.4. Alignment of the $F$ - $\pi$ Shaper

- use the alignment tools:
  - o four ball-end thrust screws on the  $F$ - $\pi$ Shaper,
  - o the screws for X/Y lateral translation on the Mount M27, to correct the displacement of the  $F$ - $\pi$ Shaper, Fig. 26,
- the criterion for proper alignment is the circular **symmetry** of the *Output Beam* profile,
- an example of an *Output Beam* profile with a correctly aligned  $F$ - $\pi$ Shaper is shown in Fig. 28.

*Note: To use the X/Y lateral translation tools ONLY !*

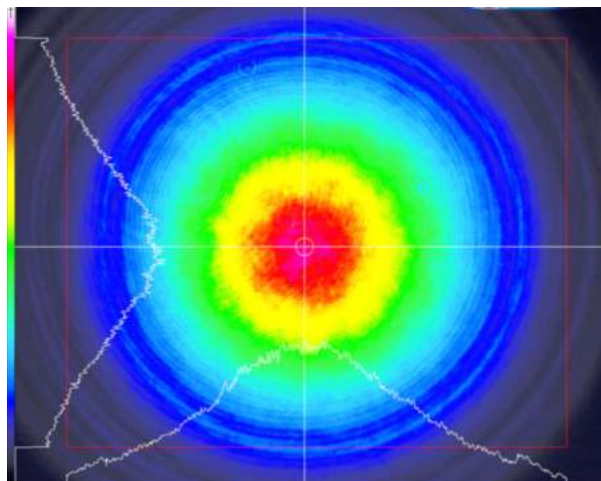


Fig. 28 Output beam profile with the aligned  $F$ - $\pi$ Shaper.

*Note: At the alignment stage, it is recommended to provide an input beam of maximum diameter, and then the beam shaping effect will be more pronounced, which simplifies the alignment process and makes it more reliable. At a late stage of the adjustment procedure, it is necessary to adjust the input beam diameter to ensure the optimum profile with minimized side-lobes in the working spot.*

To prove the optimum alignment it is necessary to analyse the focused spots in the focus area of the focusing lens.

#### 11.2.5. Alignment Lens Q

- install the *Alignment Lens Q* on the  $F$ - $\pi$ Shaper using the compatible threads M30x0.75,
- an example of mounting is shown in the photo, Fig. 29,
- install an additional neutral filter on the *Beam Profiler* to avoid damage of the camera sensor by focused laser radiation, see Fig. 30; as a rule, the optical density of this filter is 2-3Dlog,
- place the *Beam Profiler* in the area close to the focus of the *Alignment Lens Q*, and, moving the *Beam Profiler* along the optical axis, determine locations of the *Waist* and *Donut* spots; the latter is in the plane closer to the focusing lens, please refer to the sequence of profiles presented in Figs. 21 and 22,
- analysing the *Donut* spot, it is easy to check and, if necessary, correct the alignment of the  $F$ - $\pi$ Shaper.

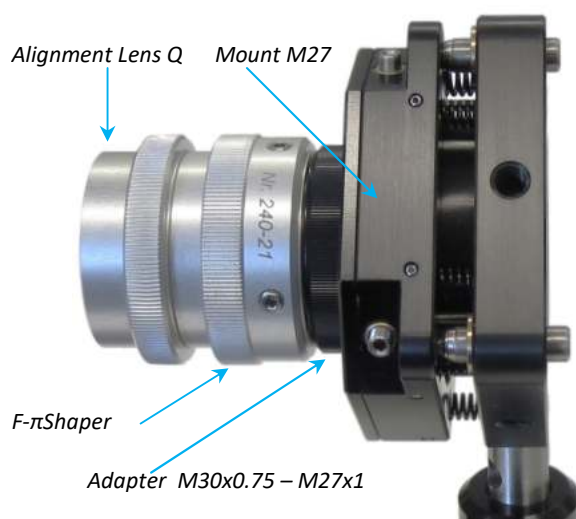


Fig. 29  $F$ - $\pi$ Shaper with the *Alignment Lens Q*, installed in the *Mount M27*.

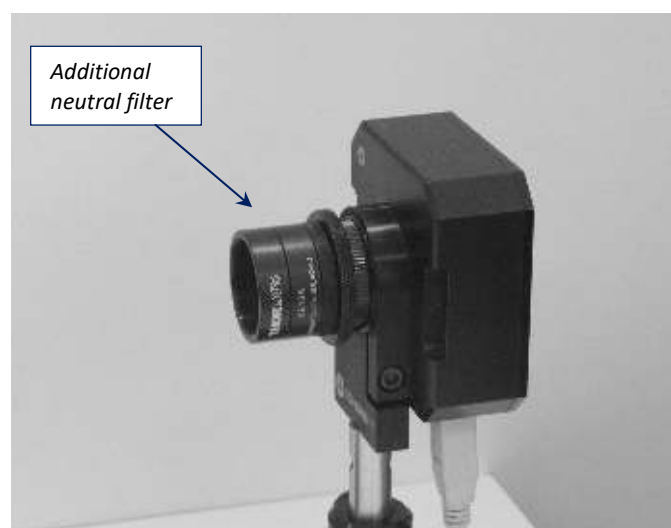


Fig. 30 Beam profiler with an additional neutral filter.

### 11.2.6. Alignment using the Donut spot

- A typical view of the *Donut spot* in the case of *F- $\pi$ Shaper* misalignment is shown in Fig. 31(a):
  - o the *F- $\pi$ Shaper* is displaced vertically downwards and horizontally to the right,
  - o majority of the spot energy is shifted upwards, to the left, where the maximum intensity is observed,
- use the alignment tools:
  - o four ball-end thrust screws on the *F- $\pi$ Shaper*,
  - o the screws for X/Y lateral translation on the Mount M27,
 to correct the displacement of the *F- $\pi$ Shaper*,

*Note: To correct the displacement of the F- $\pi$ Shaper, to move the spot in the direction of maximum intensity, in the example in Fig. 31(a), to move the Donut spot upwards and to the left.*

- the criterion of the correct alignment is the circular **symmetry** of the *Donut spot*, as shown in Figs. 2, 7, 8, 14, 21.
- an example of the *Donut spot* with a correctly aligned *F- $\pi$ Shaper* is shown Fig. 31(b).

*Note: To use the X/Y lateral translation tools ONLY !*

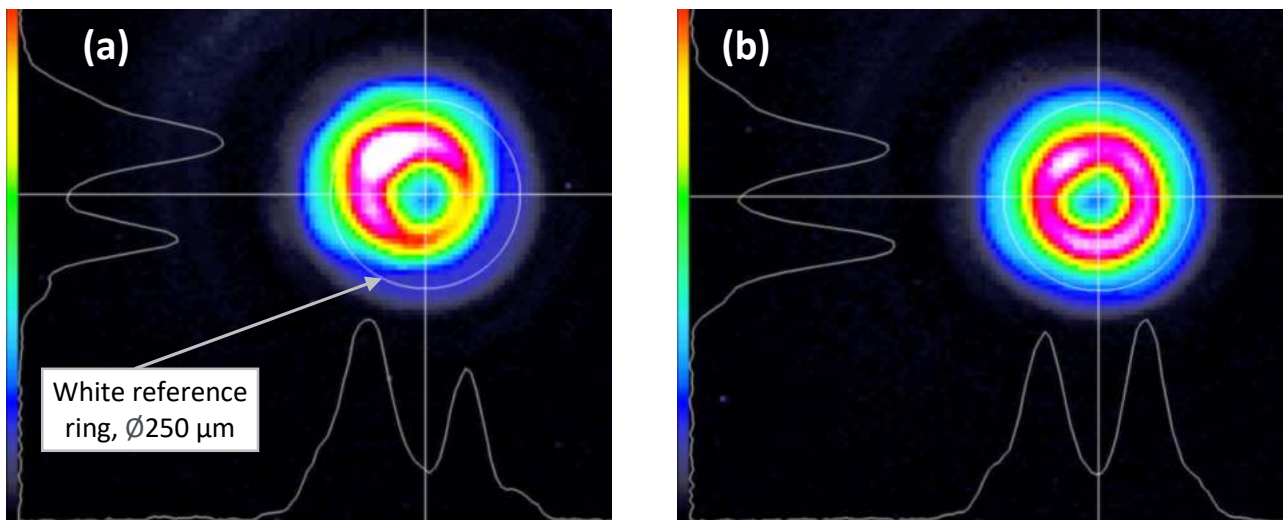


Fig. 31 Profiles of the *Donut spot* for different state of the *F- $\pi$ Shaper* alignment:

(a) misaligned *F- $\pi$ Shaper*, displacements: **vertical** downwards, **horizontal** to the right, (b) correctly aligned *F- $\pi$ Shaper*.

- Typical views of the characteristic spots *Small Flat-top* and *Flat-top in focus* with a misaligned *F- $\pi$ Shaper* are shown Fig. 32; where the *F- $\pi$ Shaper* is displaced horizontally to the left,
- In case of correct alignment, the views of the *Small Flat-top* and *Flat-top in focus* are as shown in Figs. 2, 7, 8, 14, 21, 33.

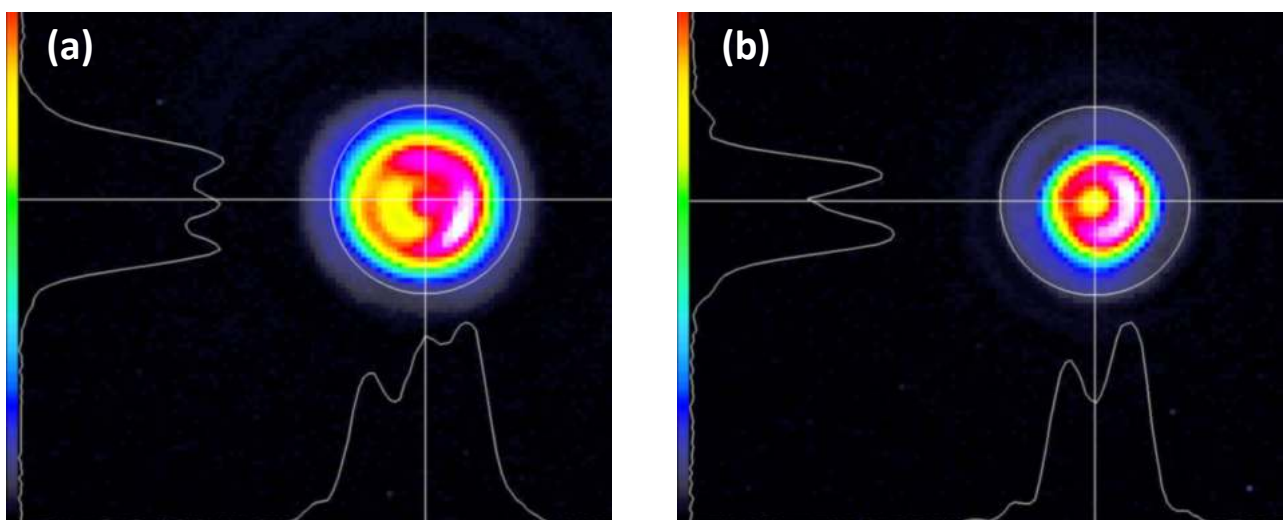


Fig. 32 Profiles of the characteristic spots in case of horizontal displacement of the *F- $\pi$ Shaper* to the left, (a) *Small Flat-top*, (b) *Flat-top* in the focal plane of the focusing lens.



### 11.2.7. Optimum input beam size

- Suppose that the *F- $\pi$ Shaper* is aligned, that is, the displacements are corrected, and the characteristic spots in the area near the lens focus are symmetrical,
- to ensure optimum profiles of the characteristic spots, for example, with minimized modulation in the *Small Flat-top* or minimized side-lobes in the *Flat-top in focus*, it is necessary to adjust the diameter of the *Input Beam* using a zoom beam expander or the method of auxiliary lens (negative or positive) described in p.4.3 of the paper “BEAM SHAPING OF FOCUSED BEAMS FOR MICROPROCESSING APPLICATIONS” in section 11.3,
- a typical criterion for the correct adjustment of the beam size is the flatness of the profile on the top of the spot *Flat-top in focus*, see the profile example in Fig. 33(c).
- as a rule, the diameter of the optimum *Input Beam* for the *Small Flat-top* is **larger** than the optimum diameter for the *Flat-top in focus*,
- examples of characteristic spots in the case of an optimum *Input Beam* diameter for the *Flat-top in focus* are shown in Fig. 33,

*Note: Adjusting the Input Beam size is the last step in the alignment procedure*

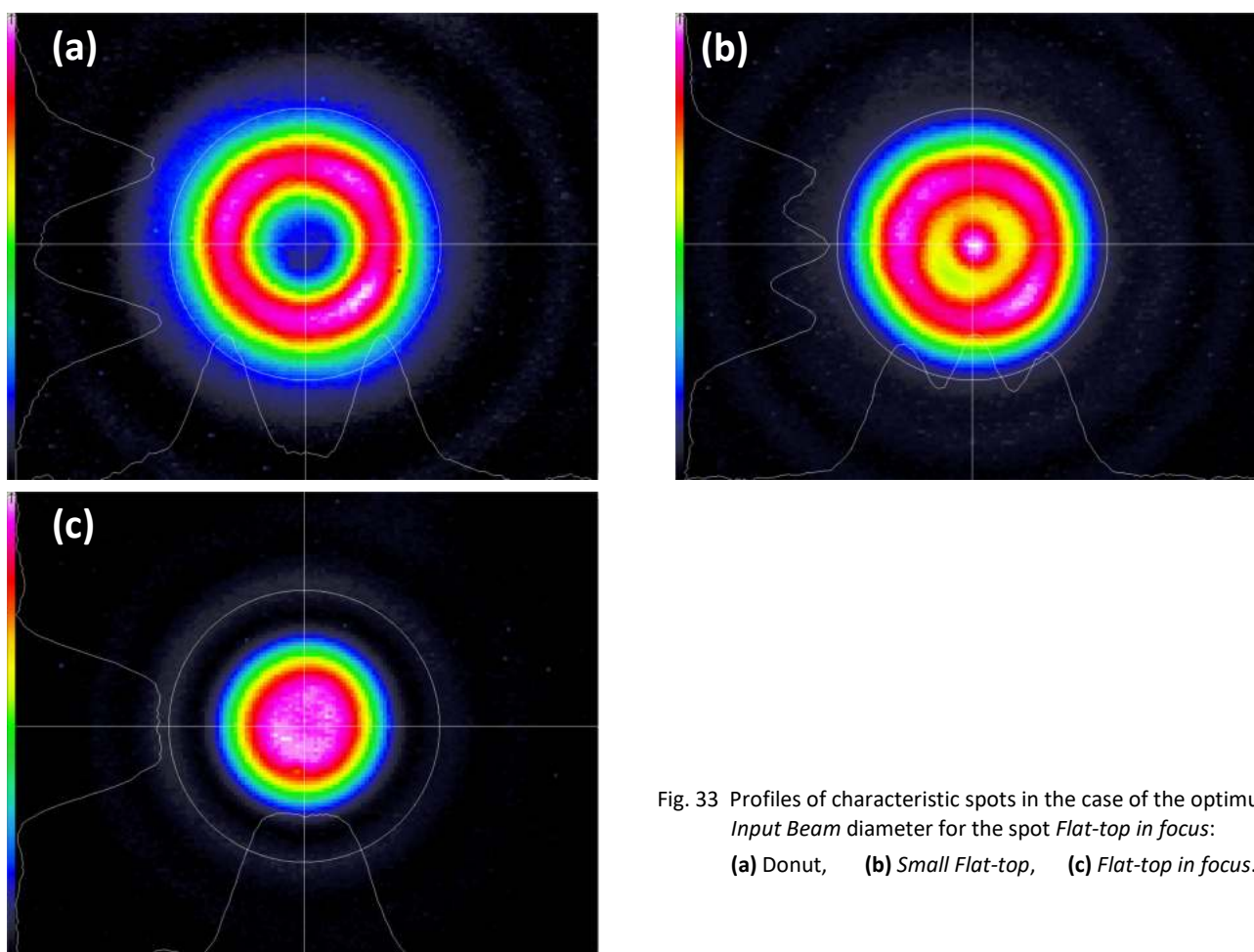


Fig. 33 Profiles of characteristic spots in the case of the optimum *Input Beam* diameter for the spot *Flat-top in focus*:  
**(a) Donut, (b) Small Flat-top, (c) Flat-top in focus.**

### 11.2.8. Normal working Focusing lens

- when the adjustment procedure of the *F- $\pi$ Shaper* is completed, the *Alignment Lens Q* should be removed, and the normal lens of the equipment should be installed in working position, then
- the profile transformation in the caustic of the focused beam will be the same as shown in Figs. 21 and 22, however
  - o the spot diameters will be reduced in proportion to the **ratio** of the focal lengths of the *Normal lens* and the *Alignment Lens Q* while
  - o reduction of the Rayleigh length, which practically defines the depth of focus (DOF), will be proportional to the **square of the ratio** of the focal lengths of the *Normal lens* and the *Alignment Lens Q*,
- for example, when switching from the *Alignment Lens Q* of 1000 mm focal length to the *Normal lens* with the focal length of 100 mm, the spots will be 10 times smaller, while the DOF 100 times (!) narrower.



### 11.2.9. Evaluation of spots profiles by material processing

When the *F- $\pi$ Shaper* is correctly aligned with the laser beam and the *Normal lens* installed in the optical system of the equipment, then the size of the resulting spots are usually less than 100  $\mu\text{m}$ , and measurements using camera-based beam profilers are not reliable. Therefore, it is recommended to test performance of a system, including alignment, by processing real materials. It is preferable to use materials with a direct correspondence of the processing result to the intensity distribution of a spot; for example, ablation of a thin film on a substrate or direct ablation of material, as shown in Fig 34.

#### Ablation of Silicon

Silicon processing is important in the semiconductor industry; Fig. 34 presents measured profiles and results of ablation at the above discussed characteristic spots:

- *Small Flat-top,*
- *Donut,*
- *Big Flat-top.*

The profile of the initial TEM<sub>00</sub> laser with  $\lambda = 1030 \text{ nm}$  and a pulse duration 8 ps is shown in Fig. 34(a), it has some imperfections (diffraction fringes) due to beam clipping in the previous optical system. Nevertheless, the intensity distributions obtained in working planes near the lens focus are close to theoretical; and the ablation process demonstrates holes with predictable sizes and depths, as well as with even edges and steep walls.

*A complete set of test data should include measurements of the entire beam caustic in the area of the lens focus with the detection of all characteristic spots shown in Figs. 21 and 22.*

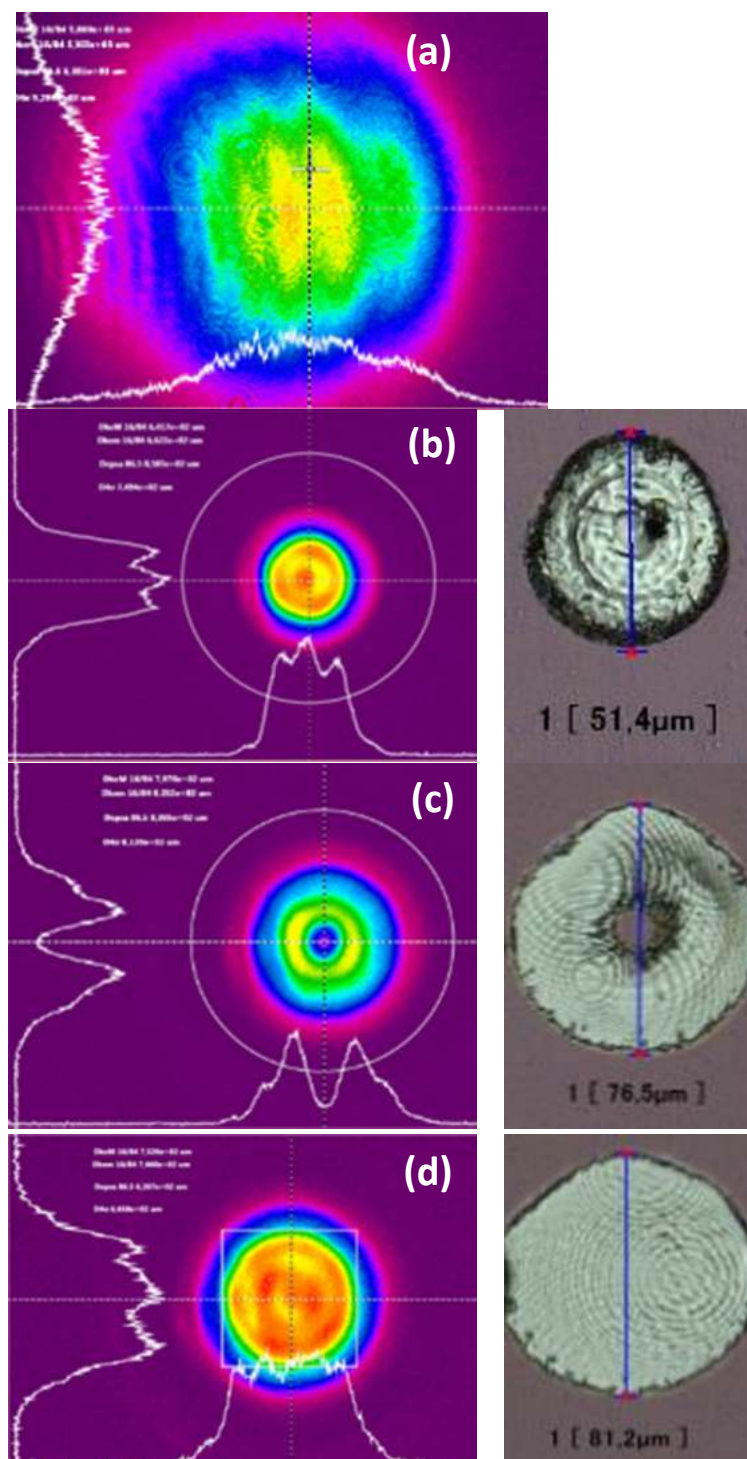


Fig. 34 Profiles of characteristic spots and Silicon ablation using a picosecond laser:

- (a) *Input Beam,* (b) *Small Flat-top,*  
(c) *Donut,* (d) *Big Flat-top,*

(Courtesy of Ernst-Abbe-Fachhochschule Jena)

### 11.3. Data for communication with a supplier

By the communication with a supplier for evaluation of the optics alignment and performance, it is recommended to present beforehand the following data measured using a beam profiler:

- Input beam
  - profile at the entrance of the *F- $\pi$ Shaper*, with numerical data for the  $1/e^2$  diameter,
  - divergence, numerical data, for example by measuring  $1/e^2$  beam diameter from the laser source at distances 50 mm, 500 mm, 1000 mm, 2000 mm,
  - astigmatism and ellipticity, numerical data,
- Output beam profile at the exit of the *F- $\pi$ Shaper* at distances 20 mm, 100 mm, see examples in Fig.20,
- Profiles in caustic by focusing using the *Alignment Lens Q* (1000 mm focal length)
  - Donut,
  - Small flat-top,
  - Waist,
  - Flat-top in focus, see examples in Figs. 21, 22,

*Do not use the Scanning Slit beam profilers!*

as well as

- Serial number of the unit, engraved on the housing,
- Main specifications of the laser:
  - wavelength,
  - CW or pulse,
  - $M^2$ ,
  - power specifications,
  - pulse energy,
  - pulse width.

Data with material processing are considered **ONLY** when the above mentioned measured profiles are presented.

*Important: No clipping or truncating the laser beam is allowed in the optical system before or after the F- $\pi$ Shaper!  
The operation physical principle presumes that the whole focused beam creates the resulting flat-top spot.  
Clipping disturbs the interference effect, leads to destroy of the resulting spot profile and diffraction side-lobes.*

## 11.4. ICALEO presentation paper

### BEAM SHAPING OF FOCUSED BEAMS FOR MICROPROCESSING APPLICATIONS

Paper P136

Alexander Laskin<sup>1</sup>, Hansung Bae<sup>2</sup>, Vadim Laskin<sup>1</sup>, Aleksei Ostrun<sup>3</sup>

<sup>1</sup> AdlOptica Optical Systems GmbH, Rudower Chaussee 29, 12489 Berlin, Germany

<sup>2</sup> ShinHoTek, #602 Uni-Tech Vil 1141-2, Baekseok 1-dong, Goyang-si, 410-837 Korea

<sup>3</sup> St. Petersburg National Research University of Information Technologies, Mechanics and Optics, Kronverkskiy pr, 49, 197101, St.Petersburg, Russia

#### 1. Abstract

Beam shaping of focused laser beams to control intensity distribution in a laser spot is important optical task in various micromachining applications like scribing, PCB drilling and others. Developing of workable optical solutions is based on diffraction theory, and one of important for practice conclusions is that flat-top intensity profile in focal plane of a focusing lens is created when the input beam has Airy-disk intensity distribution. To meet requirements of modern microprocessing machinery the beam shaping optics should be capable to operate with CW and ultra-short pulse lasers, popular F- $\Theta$  lenses and microscope objectives, galvo scanners, 3D scanning systems. All these requirements were taken into account and fulfilled while developing refractive field mapping beam shapers Focal- $\pi$ Shaper, realizing optical approach to optimize conditions of interference near the focal plane and providing variety of profiles: flat-top, donut, inverse-Gauss. Other important features are: extended depth of field similar to Rayleigh length of comparable TEM<sub>00</sub> beam, easy integration in industrial equipment, simple adjustment procedure and switching from one profile to another. Flexibility of refractive design allows implementing not only telescopic but also collimating beam shapers compatible with TEM<sub>00</sub> fiber lasers. There will be considered design basics of refractive beam shapers, examples of implementations, results of profile measurements and material processing.

#### 2. Introduction

The beam shaping optics becomes more and more popular in various laser applications; at the same time many technical solutions used in industrial laser machinery are based on applying scanning optics as versatile tools of material structuring, image recording, drilling, etc. Usually the optical systems with scanning mirror optics presume working with collimated laser beams entering the 2- and 3-axis galvo mirror scanners, and the focusing is provided by various F-theta lenses. It is well-known that focusing of a laser beam allows creating very small spots required in microprocessing applications; therefore transformation of intensity profiles of focused beams has great importance. As a solution it is suggested to apply refractive field mapping beam shapers, which principle of intensity profile transformation is based on careful manipulation of wave front of a beam with conserving the beam consistency. This approach allows creating a beam, which intensity distribution and phase front are prepared to be transformed to flat-top, inverse-Gauss or donut spots when focused by a diffraction limited lens. Since modern microprocessing applications presume applying of scanning optics we will consider beam shaper designs optimized to be applied just with scanners.

#### 3. Intensity Profile Transformation by Focusing: Theoretical considerations

Focusing of laser radiation by a lens provides concentration of laser energy in a small, typically several microns or tens of microns, laser spots. To provide such small spots, comparable with wavelengths, the focusing lenses should have diffraction limited image quality over entire working field, i.e. the residual wave aberration should be less than quarter of wavelength [4].

Behaviour of laser beam profile in zone of focal plane of a focusing lens is an important issue to be considered for practice. This analysis can be done on the base of diffraction theory, which description can be found in books [1-4], here we emphasize on some important for further consideration features.

The Huygens-Fresnel Principle is the corner stone of the diffraction theory. According to that principle each point of a wave front can be considered as a center of a secondary spherical wavelet and by the light propagating in space the distribution of light in a particular plane or a surface can be defined as result of interference of those secondary wavelets. The rigorous mathematical theory for considering the diffraction effects was built by Kirchhoff, Helmholtz, Maxwell and other scientists in 19<sup>th</sup> century, for example, usually considerations concerning particular optical effects start from so called Fresnel-Kirchhoff diffraction formula [2]. Since the integral equations of mathematical description are quite complicated and impractical for engineering purposes there are used various simplifications like Fresnel approximation or Fraunhofer approximation [2,3].

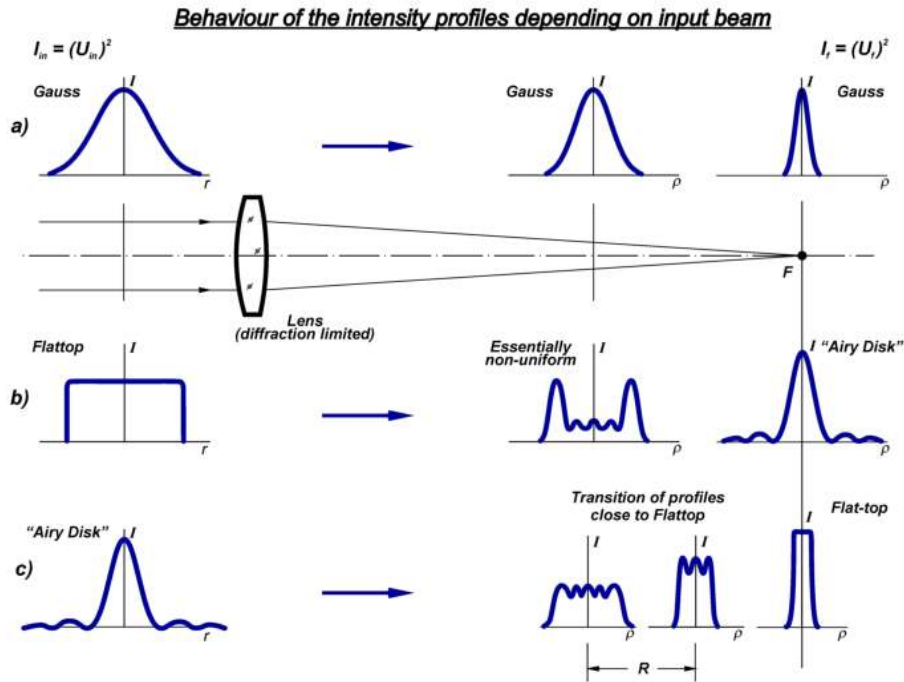


Fig. 1 Focusing of various laser beams by a lens.

case of a focal plane of a lens is proportional to Fourier-image of input field amplitude distribution; examples of this transformation are shown in Fig. 1 and will be considered later. Summarizing analytical considerations concerning the Fourier transform by an optical system of circular symmetry one can express, in polar coordinates, the field amplitude distribution  $U_f$  in the lens focal plane by equation

$$U_f(\rho) = B \int_0^{\infty} U_{in}(r) J_0(2\pi\rho r) r dr \quad (1)$$

where  $U_{in}$  is field amplitude at the lens input,  $\rho$  is polar radius in the lens focal plane,  $r$  is polar radius at the lens input,  $J_0$  is the Bessel function of the first kind, zero order,  $B$  is a constant. This expression is accordingly referred to as the Fourier-Bessel transform, or alternatively as the Hankel transform of zero order.

In most of laser technologies the result of influence of the laser radiation on material is evaluated with using intensity distribution of a beam. Therefore, for practical usage it is necessary to express the intensity distribution  $I_f$  in the focal plane of a lens through the function of field amplitude, for this purpose the well-known relationship [2] can be used

$$I_f(\rho) = [U_f(\rho)]^2 \quad (2)$$

Just the intensity distribution  $I_f$  is shown in Fig. 1 where examples of beam profile transformation are depicted.

The case of a beam focusing by a lens has great importance in considering the optical effects in various laser technologies since this is a mostly used way to create laser spots of a necessary size on a workpiece. Usually, analyzing the beam intensity profile in the focal plane of a lens is quite enough; especially when propagation TEM<sub>00</sub> laser beams is investigated. However, when an optical system contains beam shapers and intensity distribution transformation while the light propagating becomes more complicated it is necessary to consider intensity profile behavior in other zones of optical system as well, for example very important is the zone surrounding the focus of a lens.

Since the Fourier-transform is just a special case of intensity distribution description being valid for focal plane of a lens only, a complete detailed analysis of the beam profile behavior in zone of the lens focus requires applying of general mathematical descriptions of diffraction theory, for example the already mentioned Fresnel-Kirchhoff diffraction formula. Usually that interference analysis requires quite intensive mathematical computations, using special software for optical calculations. Let us omit the cumbersome mathematical computations and present here results of calculations for the cases most interesting for the practice of laser technologies:

- focusing of a TEM<sub>00</sub> (Gaussian) laser beam,
- focusing of a flat-top beam,
- creating a flat-top spot in zone of lens focus.

The results of analysis of intensity profile transformation for these cases are presented in Fig. 1 in form of graphs.

According to the Huygens-Fresnel principle, the intensity distribution in a plane of analysis is result of interference of secondary wavelets. Evidently, while the beam propagating in space the conditions for interference get changes and, hence, that pattern

varies in different planes of analysis. In other words, *in each plane after the lens the intensity profile differs from one of a neighbor plane, and features of this profile variation depends on the initial beam profile at the entrance of the lens.*

The example a) in Fig. 1 corresponds to TEM<sub>00</sub> or Gaussian beam being most popular in laser technics, the initial intensity distribution is described in polar coordinates by equation

$$I_{in}(r) = I_{in0} e^{-2r^2/\omega_0^2} \quad (3)$$

where  $I_{in}$  is intensity at the lens input,  $\omega_0$  is a waist radius of the Gaussian beam,  $I_{in0}$  is a constant.

Focusing of such a beam with a diffraction limited lens leads to creating near focal plane a spot with, again, Gaussian intensity distribution and diameter  $d$  defined by the equation

$$d = 2\omega'_0 = \frac{2\lambda f}{\pi\omega_0} M^2 \quad (4)$$

where  $\lambda$  is the wavelength,  $\omega_0$  is waist radius of focused beam,  $f$  is the lens focal length,  $M^2$  is laser beam quality factor.

Essential feature of focusing the Gaussian beam is that its intensity profile stays just Gaussian over all distance of the beam propagation, only size is varying! Result of interference for an intermediate plane (between lens and focal plane) is again the Gaussian intensity profile; this is a well-known feature widely used in laser technics,

But this brilliant feature is valid for Gaussian beams only! In case of any other profile the intensity distribution behavior differs.

This is very good seen in diagrams of the example b), Fig. 1 corresponding to the flat-top initial beam. It is a well-known conclusion of diffraction theory, described in all literature sources by considering photo or astronomic optics, that in the focal plane the intensity  $I_f$  is described by the function called as the Airy Disk

$$I_f(\rho) = I_{f0} \left[ \frac{J_1(2\pi\rho)}{2\pi\rho} \right]^2 \quad (5)$$

where  $J_1$  is the Bessel function of the first kind, first order,  $I_{f0}$  is a constant.

In the space between the lens and its focal plane the interference pattern gets strong variation both in size and in intensity distribution. One can see an essentially non-uniform profile corresponding to intermediate plane of analysis; it differs both from Airy Disk and flattop functions and is, evidently, useless for practical applications.

As we see the focusing of a flattop beam never leads to creating a spot with uniform intensity, neither in focal plane nor in intermediate planes:

*If an application needs a laser spot of uniform intensity (flat-top or top-hat), no sense to focus a flat-top beam!*

This doesn't mean, however, that a flat-top collimated beam cannot be used to create a small laser spot of uniform intensity. When an imaging approach (not focusing!) is applied, it is possible to create flat-top spots of several tens of  $\mu\text{m}$  size using imaging optical systems combined from scanning optics and additional collimating system. This technique is out of scope of this paper, some details and examples of imaging in scanning optics are considered in [6,7].

The beam focusing layout c) in Fig. 1 corresponds to very important for practice case of creating a small laser spot with uniform intensity profile just in the lens focal plane. Realizing this approach requires solving of the inverse problem – which intensity distribution should be at the entrance of a lens in order to get a flat-top spot in focal plane? This problem was, for example, discussed in paper [5]. Mathematical computations based on the inverse Fourier-transform technique give a solution that the input beam to have the intensity distribution described just by Airy Disk function, analogous to formula (5) with input beam radius  $r$  instead of  $\rho$ . Thus, *to generate a flat-top laser spot in the focal plane of a lens the input beam should have essentially non-uniform intensity distribution described by Airy disk function.*

Further analysis shows that the interference pattern in the space between the lens and its focal plane isn't constant; it gets variation both in size and in intensity distribution and flat-top and close to flat-top profiles are created not only in the focal plane but in some regions in space between the lens and its focal plane. Thus, the flattop profile in focal plane is just a special case of the continuous variation of intensity distribution and, as will be shown later the optimum, from the point of view of practice, working planes are shifted from the focal plane towards the lens. Creating of the beam with Airy Disk intensity distribution is the function of the field mapping beam shaper *Focal- $\pi$ Shaper* that operate as telescopic optical systems and can be easily integrated in optical layouts with scanning optics.

#### 4. Beam Shaping of focused beams

We discuss in this chapter refractive field mapping beam shaping optics intended to realize the above considered optical approach of creating flat-top spot in focal plane: basic design, features of using the beam shapers and some practical advices.

#### 4.1 Optical design of Focusing Beam Shaper

The refractive field mapping beam shapers like *Focal- $\pi$ Shaper* provide at the output a beam which intensity distribution is described by Airy Disk function that is an optimum one to create in focal plane of a focusing lens spot with flat-top, inverse-Gauss or donut profiles. Basic idea of the beam shaper operation is shown in Fig. 2.



Fig. 2 Principle of the *Focal- $\pi$ Shaper* operation.

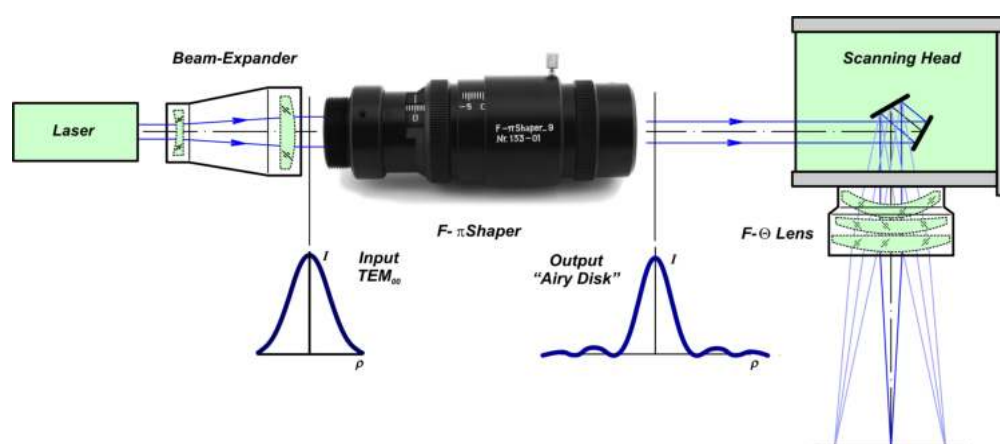


Fig. 3 Optical system with *Focal- $\pi$ Shaper* and scanning optics.

Most important features and basic principles of the *Focal- $\pi$ Shaper* are:

- telescopic refractive optical systems transforming the Gaussian to Airy Disk intensity distribution;
- flat-top, donut, inverse-Gauss and other profiles can be generated by the same device;
- operation with input  $TEM_{00}$  beams;
- operation in a certain spectral band;
- optical design without internal focusing;
- movable optical components are intended to optimize the final spot profile and to bring the plane of optimum profile in the working plane;
- compact design;
- easy integration to an optical setup and adaptation to a laser source;
- operation with any diffraction limited focusing lens;
- wide range of distances between the *Focal- $\pi$ Shaper* and the lens.

Example of optical layout of focusing the laser beam with using the *Focal- $\pi$ Shaper* and scanning optics is presented in Fig. 3. Since the *Focal- $\pi$ Shaper* operates as a telescope with magnification about  $1^x$  it can be easily integrated in existing equipment. The beam in space between the *Focal- $\pi$ Shaper* and scanning head is collimated. On the other hand, due to careful handling with wave front in the beam shaper the output profile is stable over long distance. Therefore, the distance between the *Focal- $\pi$ Shaper* and the focusing lens isn't critical; it can be chosen once but should be invariable during the system operation. Varying the beam size at the *Focal- $\pi$ Shaper* entrance leads to variation of resulting intensity profile of the final spot, therefore, varying the beam size ahead of the *Focal- $\pi$ Shaper* is a good mean to provide flat-top, donut and inverse-Gauss profiles. Choosing the plane of optimum profile and bringing it to the working plane of existing equipment is realized by internal focusing of the *Focal- $\pi$ Shaper*. Thus, the beam shaper the system can be quickly adjusted.

#### 4.2 Beam profile behaviour

The behavior of intensity distribution of a light beam is described by diffraction theory and in common case the intensity is variable when a beam propagation in space: both beam size and its intensity profile are variable. A special case is just the  $TEM_{00}$  beam: the Gaussian profile stays stable and only size is variable.



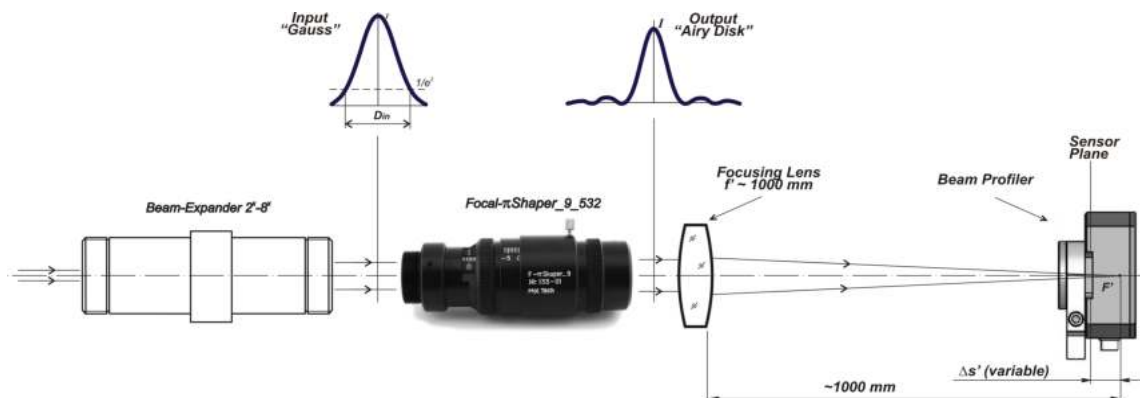


Fig. 4 Experimental optical layout to measure intensity profiles near the lens focal plane.

Since the output beam from the *Focal-πShaper* has not Gaussian but Airy disk distribution its behaviour has to be analysed using the Kirchhoff integral [2,3]. We present in this paragraph comparison of results of theoretical and experimental researches of intensity profile transformation near the focal plane of a lens. The Fraunhofer approximation of the Fresnel-Kirchhoff diffraction formula was used for theoretical calculations; experimental measurements of intensity distributions were made using a camera-based beam profiler.

The experimental setup is presented in Fig. 4: the TEM<sub>00</sub> laser beam of  $\lambda = 532\text{ nm}$  is expanded up to  $1/e^2$  diameter  $D_{in}$  at the *Focal-πShaper* entrance. Output beam with Airy disk intensity distribution is then focused by a lens of 1000 mm focal length, so the resulting laser spots have size of several hundred  $\mu\text{m}$  and can be caught by a camera-based beam profiler. Typical view of measured intensity distributions are shown in Fig. 5: top - Gaussian beam from the laser, middle - expanded beam at the *Focal-πShaper* input, bottom – beam shaper output with a characteristic ring around the central spot – this is typical pattern just for the Airy disk beams.

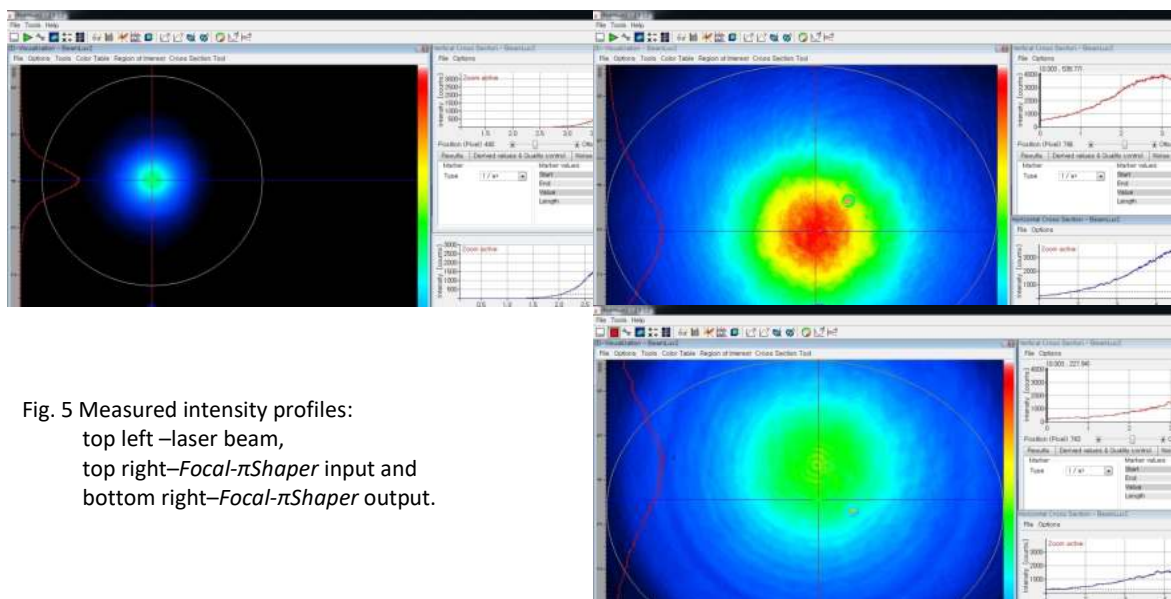


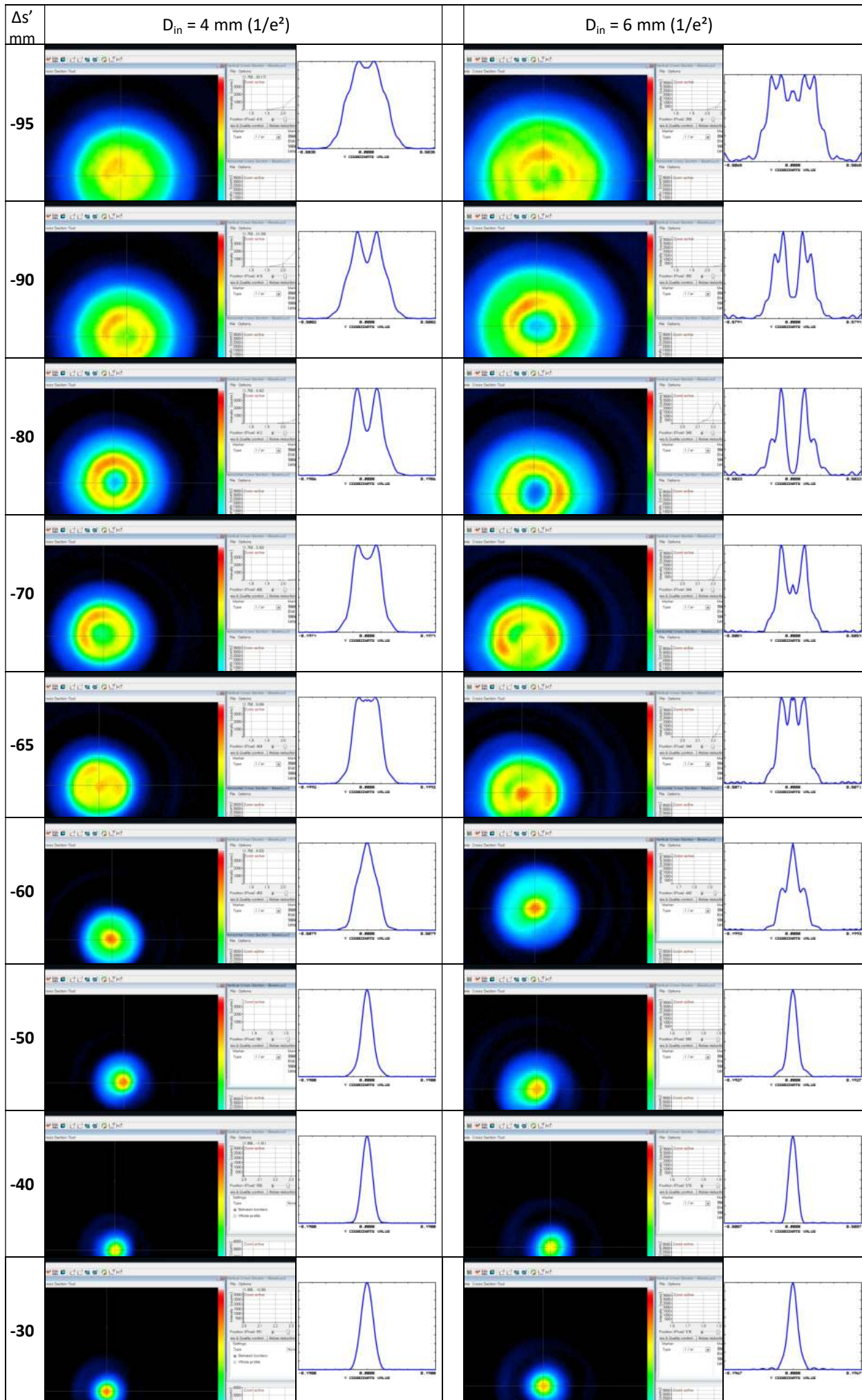
Fig. 5 Measured intensity profiles:  
 top left –laser beam,  
 top right–*Focal-πShaper* input and  
 bottom right–*Focal-πShaper* output.

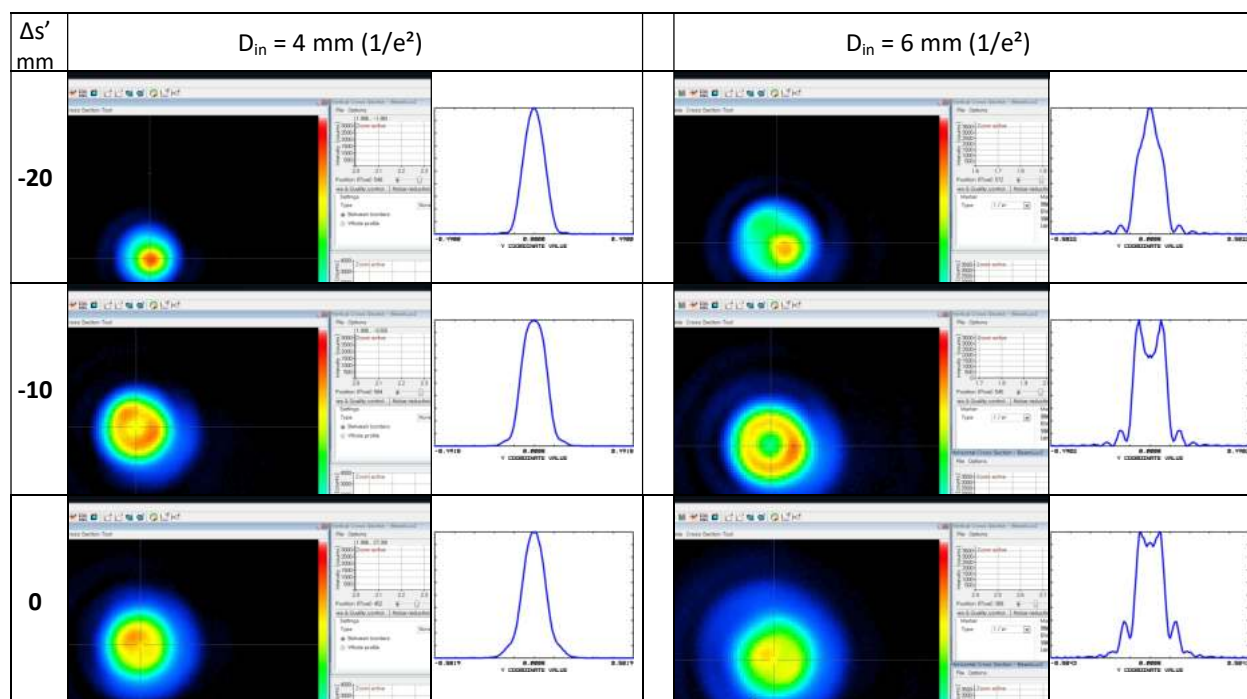
The measurements of intensity distributions are conducted for input beams with  $1/e^2$  diameter  $D_{in} = 4$  and 6 mm, the experimental distributions are combined with theoretical calculated normalized profiles and presented in Table 1 for shifts  $\Delta s'$  from focal plane. These data allow making some important conclusions about the intensity distribution behavior near the lens focus.

Comparing to an ordinary Gaussian laser beam, which size changes by focusing but intensity distribution stays unchanged and is described by the Gaussian function, the Airy beam is characterized by variation of both size and profile. According to the Huygens-Fresnel principle the intensity distribution in a certain plane is result of a beam interference: in case of Gaussian beam the result is just the Gaussian beam (the Gaussian function is the eigen function of diffraction integral), but in case of a beam after the beam shaper one can observe a sequence of interferometry patterns, and one of them is just a spot with uniform intensity is created in the lens focal plane.



Table 1 Comparison of experimental and normalized theoretical intensity distributions





One should note here that correct analysis approach presumes considering of generalized light beams and characteristics of optical systems. There are some features that are very important for further considerations:

- focus is a characterizer of a lens, one can say that the focus “belongs” to the lens, not to the beam,
- waist of Gaussian beam characterize the Gaussian beam itself (i.e. “belongs” to the beam) and the waist of a focused beam is usually close the lens focus; it is considered in practice that the beam waist coincides with the lens focal plane – this approximation is valid for lasers with short wavelengths, typically less than  $2 \mu\text{m}$ , but should be always checked when longer wavelengths, for example, for  $\text{CO}_2$  lasers,
- location of the waist of a general beam should be defined by analysis of beam profile along the optical axis; for example, as will be shown further, the waist of a focused Airy beam is shifted to the focusing lens.

The data of Table 1 show good correspondence between theoretical and experimental data, let’s consider some characteristic features of beam profile behavior.

According to the *Focal- $\pi$ Shaper* design the input beam to be Gaussian with 6 mm  $1/e^2$  diameter, therefore we consider first the data of right columns of the Table 1. The profile in the lens focal plane, corresponding to position  $\Delta s' = 0$ , is close to flat-top. Since the beam shaper provides approximation of Airy beam the theoretical resulting profile has some deviation from a perfect flat-top in form of side-lobes, while the experimental data with real laser demonstrate a flat-top spot without side-lobes but with some smoothness of spot edges, the central part of spot has uniform intensity.

When shifting the observation plane (moving the camera beam profiler) closer to the lens, the spot size is getting smaller and the intensity distribution is transformed to Gaussian-like function. In particular example the spot in position  $\Delta s' = -40$  has minimum diameter and presents the waist of the focused beam. By further shifting of the camera one can see homogenized profiles in positions  $\Delta s' = -65$  and  $\Delta s' = -95$ , as well as with inverse-Gauss and donut profiles in intermediate positions  $\Delta s' = -70$  and  $\Delta s' = -80$ . This profiles sequence “Gaussian-like - homogenized – donut – homogenized” repeats when further moving to the lens, however the spot size is growing as well, and those big spots are rarely interesting in practice and aren’t considered here. Similarly we don’t consider profiles behind the lens focus since that part of focused beam is divergent, the profiles aren’t stable and energy is spreading rapidly.

Evidently, the intensity distribution in zone of a lens focus experiences strong transformation due to essential variation of the beam phase front – the beam changes from convergent to divergent, and the front curvature is extremely high in focal plane [3]. As result the profile created in the focal plane is not stable, it is rather an interesting mathematical solution, but most often it is difficult to use that spot because of short depth of field. As will be shown later the profile in a lens focal plane becomes even more unstable in case of astigmatic laser beams that is typical for solid-state lasers. Therefore, it is usually recommended in practice to operate with spots in planes shifted to the lens where profile transformation is smoother and there exist not only homogenized profiles but also donut and inverse-Gauss that are very important in applications like welding, selective laser melting where uniform temperature profile on a workpiece is optimum.

In order to formulate practical recommendations to work with focused Airy beams we suggest to consider Fig. 6 with schematic presentation of intensity distribution transformation in two cases of beam  $1/e^2$  diameter at the *Focal- $\pi$ Shaper* entrance: 6 mm and 4 mm.

Summarizing the beam profile behavior on example of 6 mm input beam when moving the observation plane to the lens one can state:

- the spot in focal plane is flat-top,
- the beam waist with Gaussian-like profile is locating at distance  $R$ ,
- further shift at distance  $R/2$  gives a spot with uniform intensity - "small flat-top", this spot is most interesting in practice,
- in more  $R/2$  distance the donut spot is created,
- one more  $R/2$  shift gives another spot with homogenized intensity - "big flat-top".

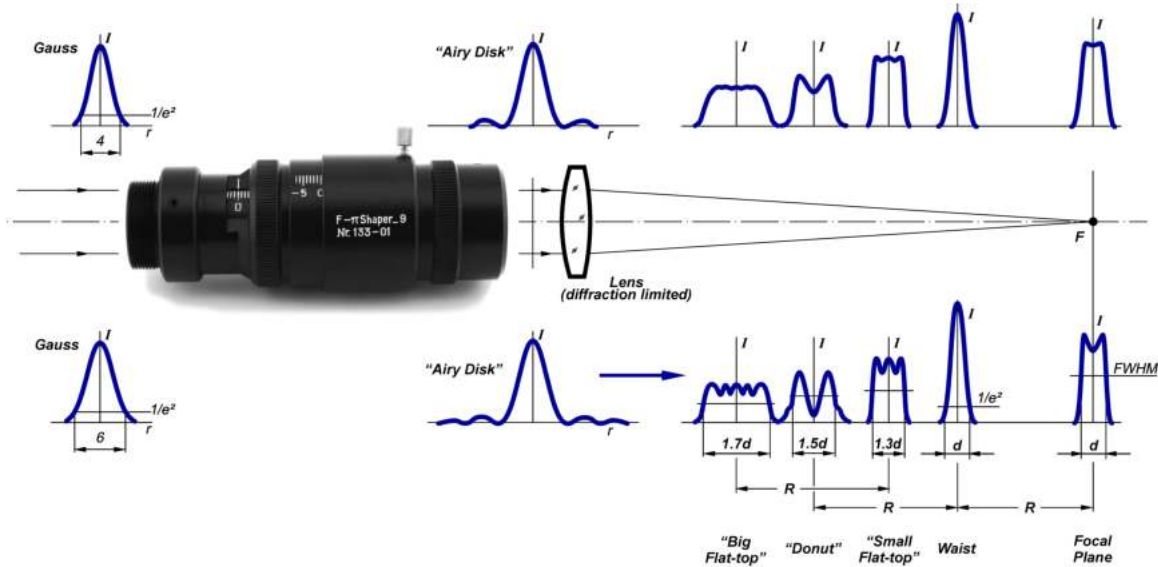


Fig. 6 To analysis of profiles by focusing the beam after *Focal-πShaper*.

That characteristic distance  $R$  is determined by properties of laser radiation, it can be expressed through Rayleigh length  $z_R$  of a reference laser beam with the same wavelength  $\lambda$  and the same divergence  $2\Theta$  using well-known formulas [3]

$$R = 2z_R = \frac{2\pi\omega_0^2}{\lambda M^2} = \frac{8\lambda M^2}{\pi(2\Theta)^2} = \frac{8\lambda f^2 M^2}{\pi D^2} \quad (6)$$

where  $M^2$  is parameter of laser beam quality,  $f$  is focal length of focusing lens,  $D$  is  $1/e^2$  diameter of the laser beam at the focusing lens and  $\omega_0'$  is waist radius of a focused Gaussian beam that is defined as

$$\omega_0' = \frac{\lambda M^2}{\pi\Theta} = \frac{2\lambda f M^2}{\pi D} \quad (7)$$

In the considered example, the diameter  $D$  is 6 mm, and the *Focal-πShaper* is a telescope with approximately  $1^\times$  magnification. The spot sizes in different positions of focused beam are shown in Fig. 6:

- the FWHM flat-top spot diameter  $d$  in the lens focal plane is equal to  $2\omega_0'$ , i.e. is the same like  $1/e^2$  diameter of the waist of the reference beam,
- $1/e^2$  waist diameter is the same like in case of focused Gaussian beam, i.e. equal to  $d$ ,
- the FWHM diameter of the „small flat-top“ is 1.3 times bigger than one in focal plane,
- the FWHM diameter of the „big flat-top“ is  $1.7d$ ,
- the FWHM diameter of the donut spot equals  $1.5d$ .

The profiles in zone of lens focus being created with 6 mm diameter input beam are acceptable in many applications, however in the interesting in practice working planes of the "small flat-top" and "big flat-top" are characterized by strong modulation of intensity. Smoother intensity distributions are achieved when input beam size is reduced; corresponding data for  $D = 4$  mm are presented in left columns of the Table 1 and in top of Fig. 6:

- intensity modulation is suppressed in "small flat-top" and "big flat-top" spots,
- intensity minimum in center of donut spot is raised,
- spot sizes and their positions are practically the same like in case of 6 mm input beam,
- edges of the spot in focal plane are smoother.

Evidently, the reduced input beam size demonstrates better performance in area of "small flat-top" to "big flat-top" spots, and provides predictable results of material processing. Indeed, in practice choosing of optimum input beam diameter depends on intensity distribution of a real laser beam that deviates from a perfect Gaussian profile. In case of the *Focal-πShaper\_9* the optimum input beam  $1/e^2$  diameters lie typically in range 4 – 5 mm.

### 4.3 Laser Beam Expansion by an Auxiliary Lens

As shown in previous paragraph variation of input beam size leads to variation of resulting profile – this is a known feature of field mapping beam shapers like *Focal-πShaper* [1]. And providing an optimum beam diameter is important while building optical systems of research setups or equipment.

A widely used approach to changing the laser beam size is applying of a beam expander. There are many commercially available models, including fixed and zoom beam expanders, motorized versions. To regret the strong competition among the beam expander manufacturers forces to reduce production costs that is achieved often through simplifying the optical design. For example, the optical systems are properly corrected to operate with axial beam only; therefore there might appear strong aberrations like coma while a beam expander tilt or internal misalignment of optical components. This isn't so "painful" when working with Gaussian beams, because due to the nature of laser radiation the energy is concentrated in a beam centre, so a Gaussian laser beam "forgives" imperfections of optical systems applied. But in case of beam shaping and careful handling with beam wavefront it is necessary to avoid any sources of wave aberrations.

Example of beam expansion of a laser beam using a commercial beam expander is presented in Fig.7.

There is evident distortion of profile in output beam that will influence on resulting intensity distribution by beam shaping of focused beam.

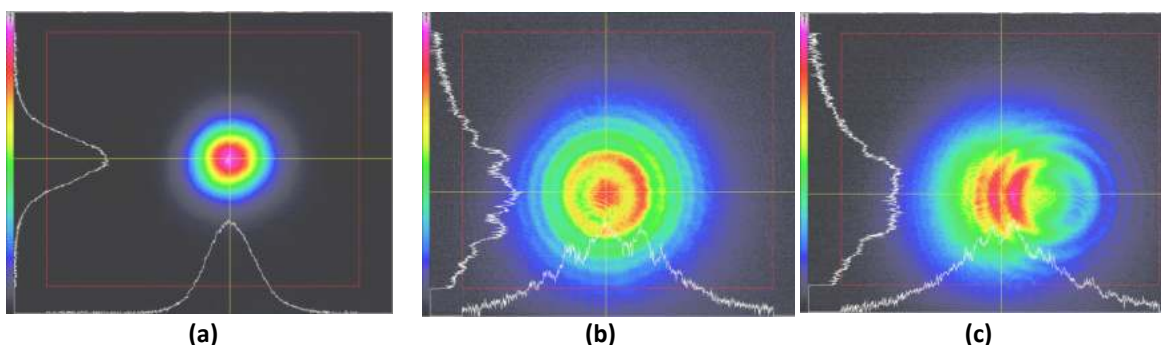


Fig. 7 Profiles by expansion of TEM<sub>00</sub> laser beam using a beam expander:  
 (a) input beam, (b) output of centered and (c) slightly tilted expander.

Therefore, when possible it is recommended to skip using a beam expander ahead of a beam shaper.

Very often by building an optical system of industrial equipment or a research setup it is possible to provide certain space between a laser and a beam shaper. This space can be used to correct the beam size by providing corresponding beam divergence: partially due to natural divergence of laser beam, partially by applying an auxiliary lens at the laser output. This approach is illustrated by layouts in Fig. 8.

Suppose a beam at a laser output has diameter  $D$  and divergence  $2\theta$ ; we consider here values at  $1/e^2$  intensity and  $D$  relates not to waist but to beam size at laser exit. The required beam diameter for a beam shaper is  $D''$ , and the distance between the laser and the beam shaper is  $L$ . Due to the natural divergence the beam has diameter  $D'$  at the beam shaper entrance, so the auxiliary Lens has to introduce certain additional divergence in order to provide the divergence angle  $2\theta'$ . One should note, the beam shaper has to be capable to compensate this resulting total input divergence angle  $2\theta'$ , then the maximum allowed angle  $2\theta'$  is defined by the beam shaper specifications, in *Focal-πShaper* it is  $\pm 5$  mrad, under some conditions  $\pm 10$  mrad.

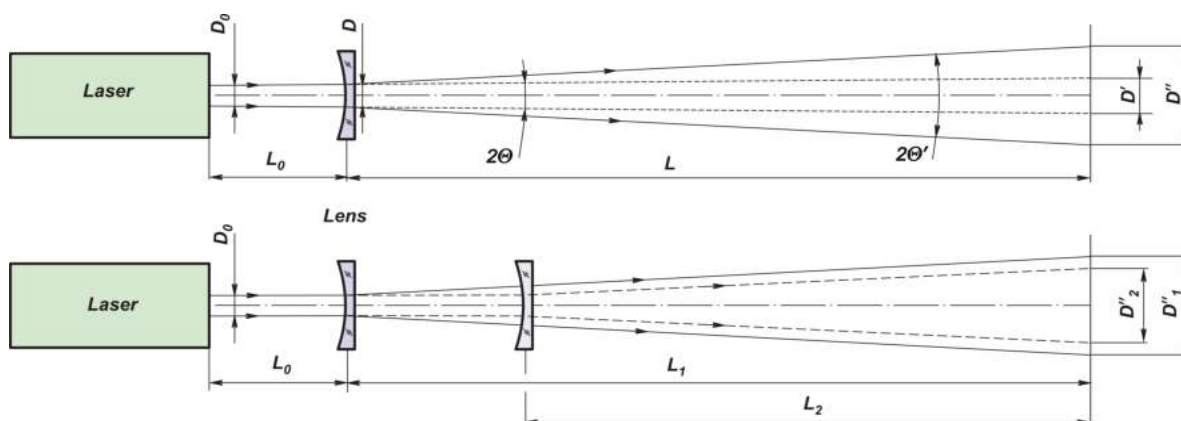


Fig. 8 Layouts to correct beam size using an auxiliary lens.



From the geometry of rays in Fig. 8, one can write

$$2\Theta' = \frac{D'' - D}{L} \quad (8)$$

$$f' = \frac{DL}{D + 2\Theta L - D''} \quad (9)$$

where  $f'$  is the focal length of the auxiliary lens.

The Eq. (8) allows evaluating required full divergence angle and check whether this correction approach is realizable with a particular beam shaper. The Eq. (9) is used to calculate the Lens focal length.

Let's consider examples:

- 1) Laser output:  $D = 1$  mm and  $2\Theta = 3$  mrad (waist  $2\omega = 0.5$  mm inside laser,  $M^2 = 1.1$ ); available length  $L = 1000$  mm; required  $D'' = 5$  mm (for *Focal- $\pi$ Shaper 9*); then  $2\Theta' = 4$  mrad – acceptable by the beam shaper,  $f' = -1000$  mm.
- 2) Laser output:  $D = 8$  mm and  $2\Theta = 0.2$  mrad; length  $L = 600$  mm; required  $D'' = 5$  mm; then  $2\Theta' = 5$  mrad – acceptable by the beam shaper,  $f' = 1538$  mm.

In both examples the auxiliary lens to be of low optical power and, hence, doesn't require precise alignment when installed in optical system. In majority of practical cases it is possible to use off-the-shelf lenses.

Moving the auxiliary lens makes it possible to tune the beam size at the beam shaper entrance; this is illustrated by layout in bottom of Fig. 8. From the geometry the resulting beam diameter  $\Delta D''$  can be defined by expression

$$\Delta D'' = D_1'' - D_2'' = (L_1 - L_2) \frac{2\Theta L_2 - D_1}{f'} \quad (10)$$

Thus, when certain air gap after a laser is available the optimum input beam diameter for a beam shaper can be adjusted using a single off-the-shelf lens.

#### 4.4 Alignment

As optical devices designed to work with axial beams the refractive field mapping beam shapers operate in relatively narrow angular field, therefore one has to take care for their proper alignment with respect to a laser and other components of an optical system. Due to optical design implementation the *Focal- $\pi$ Shapers* aren't sensitive to misalignments - typical tolerances are characterized by lateral translation error 0.1 mm and tilt of 5 arcmin with respect to laser beam. Evidently, these tolerances aren't tough and can be provided using ordinary 4-axis mounts. To quicken the alignment procedure it is usually recommended to apply alignment tools like ones described in [8].

Pointing laser beam instability should be analyzed while the beam shaper alignment. It is common to perform adjustments at low power operation mode of the laser to provide safe work conditions and prevent damaging of tools like beam profilers, filters, etc.; then the laser is switched in full power mode for a process. Due to features of laser design there might be deviation of a beam while switching between the low and full power operation modes that would inevitably lead to essential lateral shift of the beam at a beam shaper entrance. This effect becomes more pronounced in case of long air gap between laser and beam shaper, and is very critical for solid-state lasers. Example of this lateral shift is illustrated in Fig. 9: when switching laser power from 0.5 W (left) to 10 W (right) while distance from laser to the *Focal- $\pi$ Shaper* is 3.5 meter there appears a lateral shift of about 1 mm (!) - this is essential misalignment that results strong distortion of final spot profile.

To avoid this misalignment it is recommended to perform adjustments in full power mode and use beam profilers with dedicated attenuators.

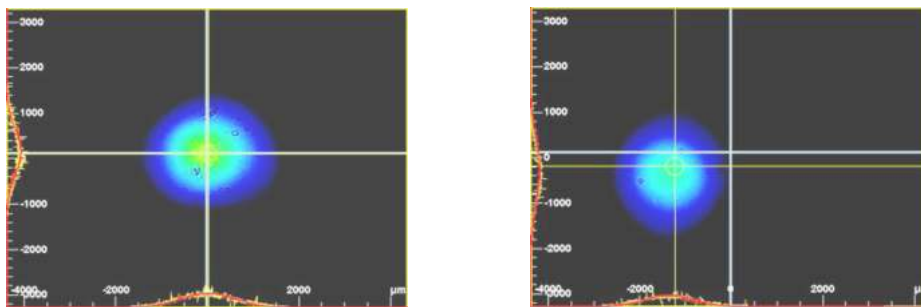


Fig. 9 Pointing error of solid-state laser: *left* – low power, *right* – full power operation modes.



#### 4.5 Influence of astigmatism of input beam

Astigmatism is a physical effect when a focused beam has two separate focuses for two orthogonally related sections, usually meridional and sagittal ones [3, 4]. A laser beam can become astigmatic because of laser design itself, variation of operation parameters (current on pumping laser diodes, repetition rate, pulse duration, etc.) as well as due to astigmatism induced by components of optical system (mirrors, lenses). Astigmatism is an inherent property of radiation of some types of solid state lasers; it is usually suppressed in modern lasers for determined parameters of operation through optimisation of their design, but appears when parameters deviation from those optimum values. Fiber laser and fiber-coupled lasers demonstrate usually weak astigmatism.

Most often astigmatic beams have elliptic shape; it is also possible when a wide collimated beam of several millimetres or centimetres diameter is round but is inherently astigmatic. A simple and effective way to visualize and evaluate astigmatism is the beam focusing and analysis of intensity profiles around the beam waist. Example of profiles before, after and in waist of focused slightly astigmatic Gaussian laser beam is presented in Fig.10:

- the spots before and after the waist are elliptic,
- their long axis are turned at 90° - this is typical behaviour of astigmatic light beams,
- the spot in waist is round.

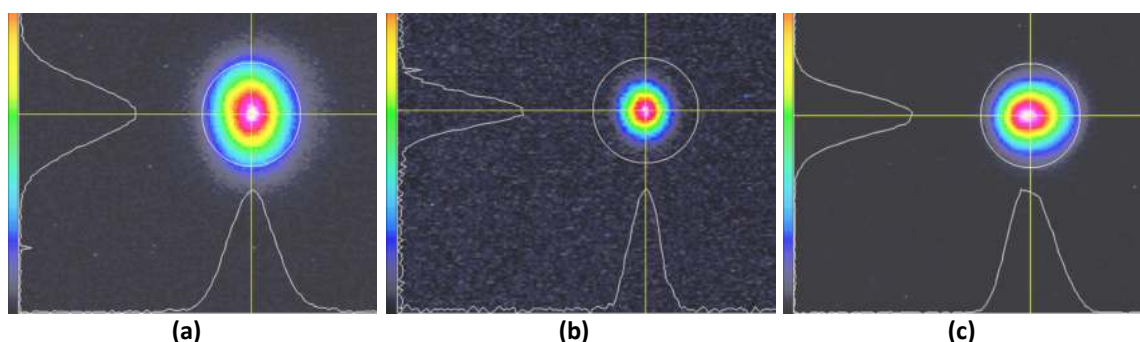


Fig. 10 Profiles by focusing of astigmatic laser beam: (a) before waist, (b) in waist and (c) behind waist.

When working with an ordinary Gaussian beam the influence of astigmatism on a process is not strong, since the spot in the waist is round and certain increasing of its diameter doesn't bring essential change in result of processing. But in case of beam shaping of focused beam astigmatism leads to characteristic change of resulting profile – the circular symmetry of intensity distribution is lost and section profiles have different view. Example of flat-top spot in the lens focal plane is shown in

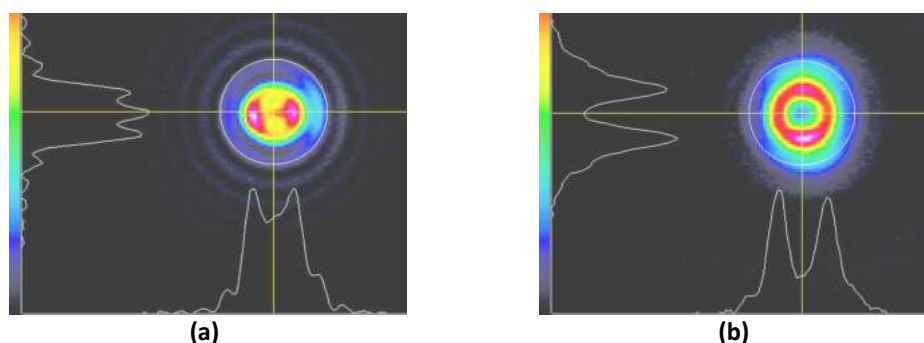


Fig. 11 Profiles of focused astigmatic beam: (a) – flat-top in focal plane, (b) – donut shape.

Fig. 11 (a); in many applications it is possible to work with such a spot and get acceptable processing results, but the unsymmetrical intensity profile has to be taken into account.

Interesting fact is that even in case of astigmatic laser beam the donut spot demonstrates regular round shape, Fig. 11 (b). This feature can be used to simplify the alignment procedure – when a beam shaper is aligned using 4-axis mount it is recommended to put a beam profiler just in the plane of donut spot and use round shape of profile as a criterion of proper alignment.

Astigmatism can be also introduced by components of optical path: lenses, beam expanders, mirrors. Therefore, it is always advisable to simplify the optical system, for example to avoid using of beam expanders as discussed in previous paragraphs.

#### 4.6 Notes to work with F- $\theta$ lenses

The considered beam shapers for focused beams are intended to be used with any diffraction limited lens, which wave aberration doesn't exceed  $\lambda/4$  value over whole working field. Majority of commercially available widely used in industrial application F- $\theta$  lenses fulfil this condition, there are however some features relating to their optical design.

F- $\theta$  lenses present multi-lens optical systems providing flat working field – the lens focal plane. Therefore the focal length of

an F- $\Theta$  lens isn't constant over whole working field, it depends on the field angle. In popular lenses this focal length difference from the field centre to periphery reaches 10-15%; this variation can be detected by analysing effective spot sizes even with ordinary TEM<sub>00</sub> beam.

As shown in previous paragraphs the intensity distribution of focused Airy beam near the lens focus depends on the lens focal length and distance from the focal plane. Therefore there exists certain variation of spot sizes and profiles for spots in centre and periphery of working field. Usually this effect isn't strong but has to be taken into account while evaluation of results of processing.

Telecentric F- $\Theta$  lenses have less variation of focal length, and its influence is practically negligible.

### 5. Experimental Results of Microprocessing

Even edges and reduced heat affected zone (HAZ) are common aims in various micromachining applications. Beam shaping and providing flat-top or other intensity profiles of the laser spot (donut, inverse-Gauss) is one of key techniques of improving those applications, and using the *Focal- $\pi$ Shaper* brings flexibility in realization of these techniques. We present in this chapter some results of material processing.

#### 5.1 Scribing on glass

The optical layout presented in Fig. 3 was used to improve laser scribing of glass using TEM<sub>00</sub> ultrashort pulse laser to create trenches of 6-7 microns width. Comparison of results of scribing with a pure TEM<sub>00</sub> laser beam and with *Focal- $\pi$ Shaper 9\_1064* installed ahead of the scanning head is presented in Fig. 12.

The difference in quality of scribing is evident: irregular trench edge and wide HAZ in case of TEM<sub>00</sub> beam, and even trench edges, steep walls and practically absent HAZ when *Focal- $\pi$ Shaper* is used.

Evidently, with using the *Focal- $\pi$ Shaper* it is possible to enhance the quality and reliability of scribing process.

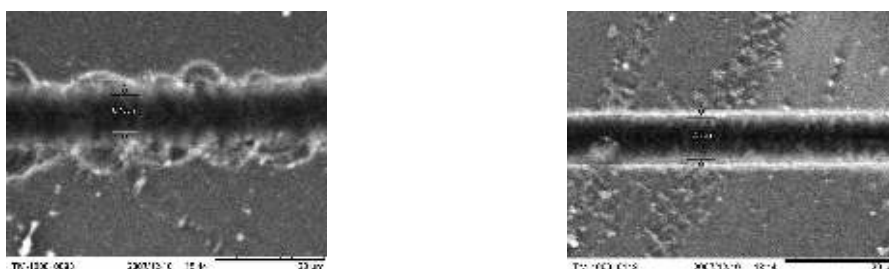


Fig. 12 Scribing by TEM<sub>00</sub> femtosecond Laser: *left* - TEM<sub>00</sub> laser beam, *right* - after the *F- $\pi$ Shaper* (Courtesy of Altechna)

#### 5.2 Scribing of thin-film material

Laser scribing of thin layers is widely used in photovoltaics technologies, patterning in display production and many others. Example of realization of this technique to ablate 210 nm thin film of photovoltaics material is shown in Fig. 13, where

- top screenshot presents initial profile of UV laser ( $\lambda=343$  nm, pulse duration 500 fs),
- the central screenshot shows profile of flat-top spot near focal plane of F- $\Theta$  lens,
- view of the resulting trench of 40  $\mu$ m width (100<sup>x</sup> microscopy) is shown in bottom left picture, and
- profile measurements for the resulting trench are presented in bottom right pictures.

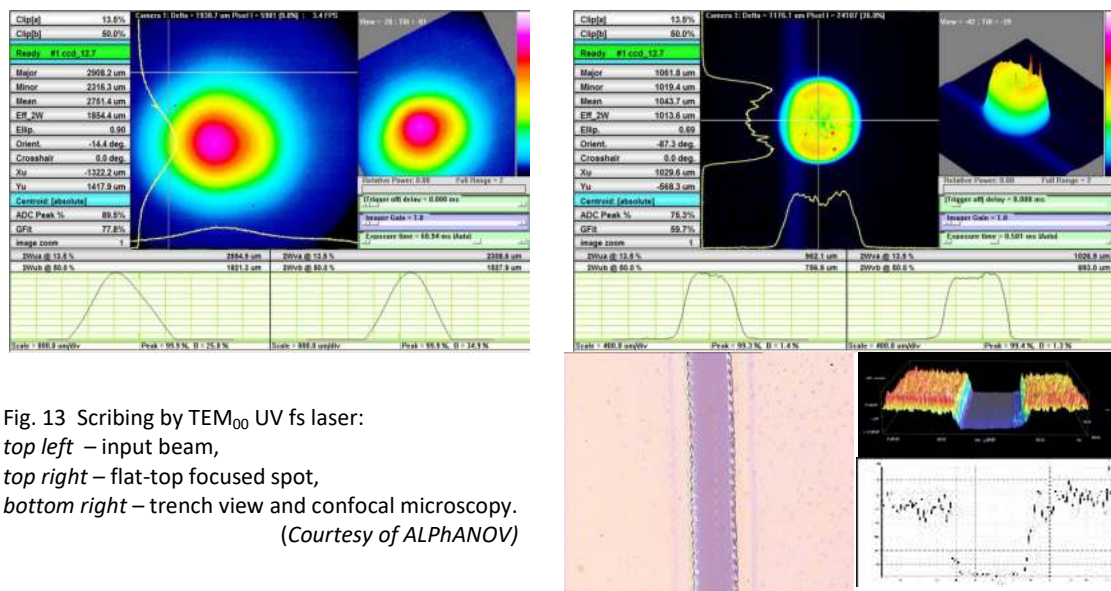


Fig. 13 Scribing by TEM<sub>00</sub> UV fs laser: *top left* – input beam, *top right* – flat-top focused spot, *bottom right* – trench view and confocal microscopy. (Courtesy of ALPhANOV)

The initial laser beam is astigmatic, therefore the resulting flat-top spot, Fig. 13, centre, has difference of intensity distribution in vertical and horizontal directions. Nevertheless, it is possible to reach high quality trench of 40  $\mu\text{m}$  width with steep edges and not damaged beneath layer.

### 5.3 Ablation of Silicon

Processing of silicon is important in microelectronics, Fig. 14 presents measured profiles and results of ablation in earlier discussed three characteristic spots: “small flat-top”, donut, “big flat-top”. The profile of initial TEM<sub>00</sub> laser with  $\lambda = 1030$  nm and pulse duration 8 ps is shown in Fig. 14 (a), it has some imperfections (diffraction fringes) due to beam clipping in previous optical system, nevertheless the resulting intensity distributions in working planes near the lens focus are close to theoretical ones, and the ablation process demonstrates holes with predictable sizes and depths as well as with even edges and steep walls.

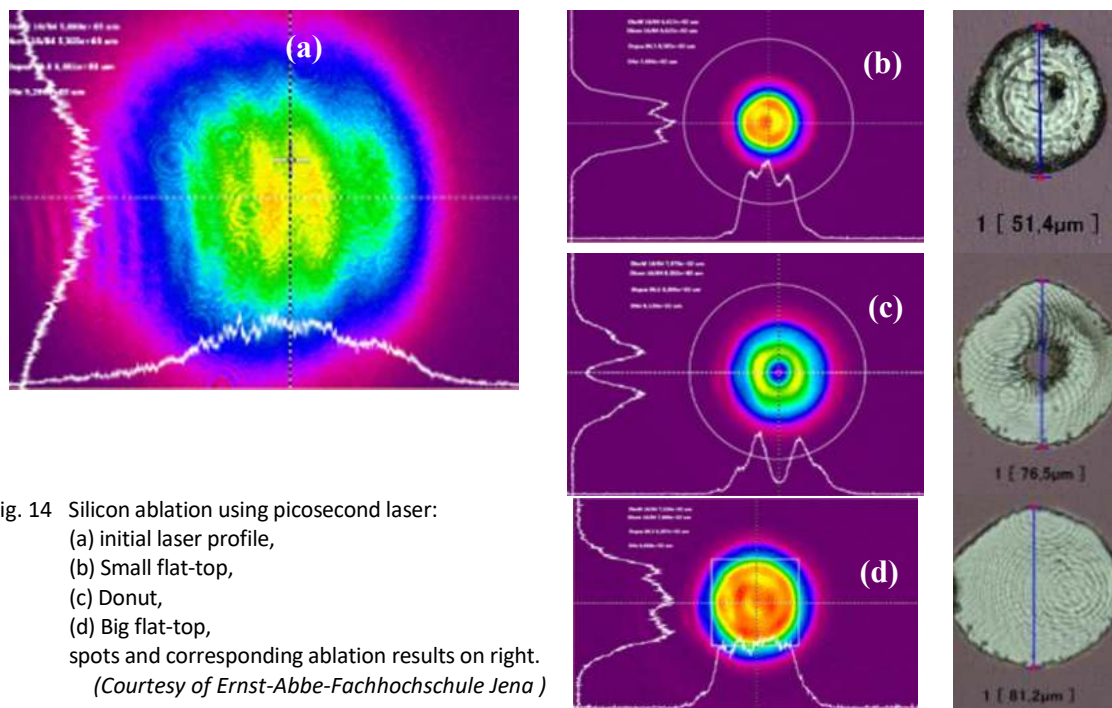


Fig. 14 Silicon ablation using picosecond laser:  
 (a) initial laser profile,  
 (b) Small flat-top,  
 (c) Donut,  
 (d) Big flat-top,  
 spots and corresponding ablation results on right.  
 (Courtesy of Ernst-Abbe-Fachhochschule Jena)

## 6. Conclusions

Refractive beam shapers of field mapping type transforming a Gaussian beam to a beam with Airy disk intensity distribution provide assured beam shaping of focused laser beams and creating spots with flat-top, inverse-Gauss and donut profiles. The data presented demonstrate good correspondence of theoretical and experimental data. The considered examples of this type of beam shaping in micromachining techniques confirm its applicability in scientific and industrial applications.

## 7. References

- [1] Dickey, F.M. (2014) Laser Beam Shaping: Theory and Techniques 2nd edn., CRC Press.
- [2] Goodman, J.W. (1996) Introduction to Fourier Optics, McGraw-Hill.
- [3] Born, M. and Wolf, E. (1999) Principles of Optics 7th edn., Cambridge University Press.
- [4] Smith, W.J. (2000) Modern Optical Engineering, McGraw-Hill, New York.
- [5] Kanzler, K. (2001) Transformation of a gaussian laser beam to an Airy pattern for use in focal plane intensity shaping using diffractive optics: Proc. SPIE 4443, Paper 4443-09.
- [6] Laskin A., Laskin V. (2010) Refractive field mapping beam shaping optics: important features for a right choice: Proc. ICALEO.
- [7] Laskin A., Šiaulytis N., Šlekys G., Laskin V. (2013) Beam shaping unit for micromachining: Proc. SPIE 8843, Paper 88430G .
- [8] Manual: Recommended alignment [http://www.adloptica.com/manual/Alignment\\_pish66\\_f\\_pish9.pdf](http://www.adloptica.com/manual/Alignment_pish66_f_pish9.pdf).

## Acknowledgement

The authors thank M. Chanal and L. Wipliez from ALPHANOV, France, C. Schindler from Ernst-Abbe-Fachhochschule Jena, G. Šlekys from Altechna, Lithuania and J. Chen from Arno Electro-Optics, Taiwan for their active and patient work with optics discussed in this paper and kind permission to publish some results achieved during their experiments.